Review

Small direct methanol fuel cells with passive supply of reactants

T.S. Zhao*, R. Chen, W.W. Yang, C. Xu

Department of Mechanical Engineering, The Hong Kong University of Science and Technology, Clear Water Bay, Kowloon, Hong Kong SAR, China

ARTICLE INFO

ABSTRACT

Small, stand-alone, direct methanol fuel cells (DMFCs) that have no auxiliary liquid pumps and gas blowers/compressors are known as passive DMFCs. The devices are ideal for powering portable electronic devices, as this type of fuel cell uniquely has a simple and compact system and no parasitic power losses. This article provides a comprehensive review of experimental and numerical studies of heat and mass transport in passive DMFCs. Emphasis is placed on the mechanisms and key issues of the mass transport of each species through the fuel cell structure under the influence of passive forces. It is shown that the key issue regarding the methanol supply is how to feed high-concentration methanol solution but with minimum methanol crossover through the membrane so that both the system specific energy and cell performance can be maximized. The key issue regarding the oxygen supply is how to enhance the removal of liquid water from the cathode under the air-breathing condition. For water transport, the aim is to transport the water produced on the cathode through the membrane to the anode by optimizing the design of the membrane electrode assembly so that the fuel cell can be operated with pure methanol and with minimum flooding at the cathode. The heat loss from a passive DMFC is usually large and it is therefore critically important to reduce this feature so that the fuel cell can be operated at a sufficiently high temperature, which critically affects the cell performance.

© 2009 Elsevier B.V. All rights reserved.

Contents

* Corresponding author. Tel.: +852 2358 8647; fax: +852 2358 1543.
   E-mail address: metzhao@ust.hk (T.S. Zhao).

1. Introduction

A direct methanol fuel cell (DMFC) directly converts the chemical energy stored in methanol to electricity. Because of its simplicity, high-specific energy, instantaneous recharging and presumably long life, the DMFC has been identified as one of the most promising candidates to replace batteries in micropower applications. Like other types of fuel cell, the core of the DMFC system is the electrodes, electrolyte and flow-fields. Other parts of the fuel cell system, such as the auxiliary systems for the supply/removal of reactants/products, can also critically affect the performance, operating stability and durability of the fuel cell, as well as its suitability for specific applications. Over the past decades, extensive efforts have been made to the study of the DMFCs with the active supply of the liquid fuel by means of liquid pumps and oxygen/air by means of gas blowers/compressors [1–19]. The addition of these auxiliary devices makes the overall fuel cell system more bulky and complex, reducing not only the volumetric energy density but also the design flexibility when the required size of the fuel cell system is small. More importantly, the added pumps, and blowers/compressors consume electricity generated by the fuel cell, thereby increasing parasitic energy losses and lowering the overall efficiency of the system. In order to make the DMFC more competitive with conventional battery technologies, the concept of a passive DMFC, which has no auxiliary liquid pump and gas blower/compressor but relies on diffusion and natural convection to supply the fuel and oxygen, was proposed and extensively investigated [20–59]. Although the passive DMFC generates lower output power than does the active DMFC, it is still the best choice for portable-power applications in which the simplicity of diffusion and natural-convection reactant delivery outweighs the cost, limited lifetime, reliability, complexity, noise, volume, weight, and parasitic power losses.

The purpose of this review is to summarize recent advances in the development of passive DMFCs and to provide an outlook for future research directions. Emphasis is placed on elaborating the mechanisms and key issues of mass transport of each species through the fuel cell structure under the influence of passive forces. The remainder of the review is organized as follows: Section 2 gives a general description of the DMFC with the passive supply of reactants; Section 3 discusses about the critical issues associated with the passive fuel and oxygen supply; Sections 4 and 5 examine past efforts on the mass transport of methanol with low- and high-methanol concentrations, respectively; Section 6 evaluates the high-concentration
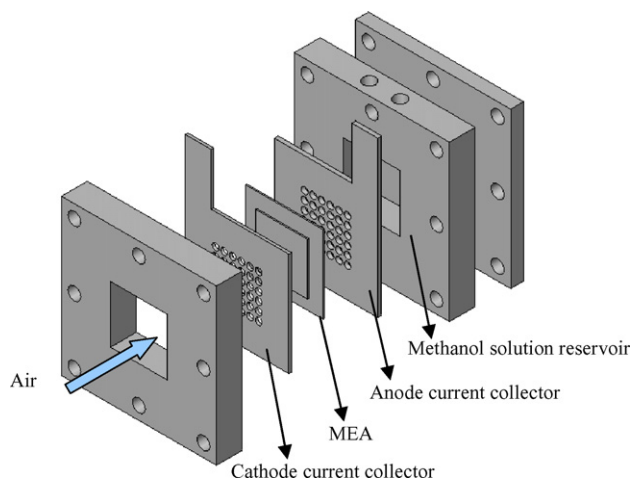

Fig. 1. Schematic of passive direct methanol fuel cell.

Nomenclature

C	molar concentration ($mol\,m^{-3}$)
D	diffusivity ($m^2\,s^{-1}$)
F	Faraday constant ($96478\,C\,mol^{-1}$)
G	Gibbs free energy ($kJ\,mol^{-1}$)
H	enthalpy ($J\,mol^{-1}$)
h	heat or mass transfer coefficient ($W\,m^{-2}\,K^{-1}/mol\,m^{-2}\,s^{-1}$)
h_v	latent heat of vaporization of liquid water ($kJ\,mol^{-1}$)
i	current density ($A\,m^{-2}$)
i_p	internal current density ($A\,m^{-2}$)
J	Levertte function
K	permeability of porous material (m^2)
k_r	relative permeability
l	thickness (m)
M	molar weight ($g\,mol^{-1}$)
N_{cross}	flux of methanol through the membrane ($mol\,m^{-2}\,s^{-1}$)
N_{H_2O}	flux of water through the membrane ($mol\,m^{-2}\,s^{-1}$)
n_d^m	electro-osmotic drag coefficient of methanol
n_{H_2O}	electro-osmotic drag coefficient of water
R	gas constant ($J\,mol^{-1}\,K^{-1}$)
q	heat generation rate ($W\,m^{-2}\,s^{-1}$)
R_w	interfacial transfer rate of water ($mol\,m^{-3}\,s^{-1}$)
s	liquid saturation
T	temperature (K)

Greek letters

α	charge transfer coefficient
ε	porosity of porous medium
η	overpotential (V)
λ	effective thermal conductivity ($W\,m^{-1}\,K^{-1}$)
θ_c	contact angle (°)
μ	viscosity ($kg\,m^{-1}\,s^{-1}$)
ρ	density ($kg\,m^{-3}$)
σ	surface tension ($N\,m^{-1}$)

Superscript

eff	effective value
ref	reference value

Subscript

a	anode
acl	anode catalyst layer
c	cathode
cc	current collector
ccl	cathode catalyst layer
dl	diffusion layer
g	gas phase
l	liquid phase
m	methanol
mem	membrane
O_2	oxygen
v	water vapor

methanol supply system; Section 7 reviews water and oxygen transport in the passive DMFC; Section 8 focuses on the heat transport in passive DMFCs; past efforts to develop passive DMFC stacks are considered in Section 9; Section 10 discusses the modelling of passive DMFCs; finally, a summary is given in Section 11.

2. General description of passive DMFC

Fig. 1 illustrates a typical design of passive DMFC, which consists of a fuel reservoir, an anode current-collector (CC), a membrane electrode assembly (MEA), and a cathode current-collector. The MEA for the passive DMFC is similar to that for active DMFCs and, as shown in Fig. 2, is composed of an anode diffusion layer (DL), an anode catalyst layer (CL), a polymer electrolyte membrane (PEM), a cathode diffusion layer (DL), and a cathode catalyst layer (CL). The function of the membrane is to conduct protons from the anode to the cathode, and to serve as a separator between these two electrodes. Typically, perfluorinated sulfonic acid ion-exchange membranes, developed by DuPont and trademarked as Nafion®, are used for passive DMFCs. The function of each DL is to provide a support to the corresponding CL, to distribute reactants over the CLs, and to conduct electricity to the current-collectors. The DLs at both the anode and cathode (ADL and CDL, respectively) usually consist of two layers, a backing layer (BL) that is made of carbon cloth or carbon paper, and a micro-porous layer (MPL) that is composed of a hydrophobic polymer and carbon powder. Different from the DLs, both CLs are made of catalysts mixed with an ionomer to provide triple-phase boundaries for the methanol oxidation reaction at the anode and the oxygen reduction reaction at the cathode.

The transport mechanisms of the passive supply/removal of reactants/products in the passive DMFC are shown in Fig. 2. Since the anode electrode is directly in contact with the methanol solution in the fuel reservoir, methanol and water are transported from the reservoir to the anode CL mainly by diffusion due to the concentration difference between the fuel reservoir and the anode CL [24]. Concurrently, in the fuel reservoir natural convection as a result of the density difference between the liquid solution and CO_2 that is generated in the anode CL and the temperature decrease from the electrode toward the fuel reservoir also assists the methanol transport from the bulk solution to the anode DL surface. In the anode CL, part of methanol is oxidized to generate electrons, protons, CO_2 and heat as follows:

$$CH_3OH + H_2O \rightarrow CO_2 + 6H^+ + 6e^- + heat \qquad (1)$$
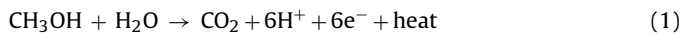
while the remainder of methanol may permeate the membrane, arrive at the cathode, and be oxidized there to create a so-called mixed potential and hence decrease the cell voltage. The CO_2 generated in the anode CL is then transferred back to the fuel reservoir by the gas pressure difference and by the buoyancy force in the fuel reservoir. On the cathode, since the electrode is directly exposed to ambient, oxygen is transported from the air to the cathode DL surface, not only by diffusion due to the oxygen concentration difference but also by natural convection arising from the temperature difference between the cathode and ambient air [24]. The oxygen transport from the cathode DL surface to the cathode CL is mainly by diffusion due to the oxygen concentration difference. In the cathode CL, part of the oxygen reacts with the protons that are conducted through the membrane from the anode and the electrons that come from the external circuit to form water and heat as follows:

$$6H^+ + 6e^- + 3/2O_2 \rightarrow 3H_2O + heat \qquad (2)$$
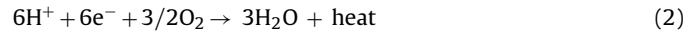
while the remaining oxygen electrochemically reacts with the permeated methanol to produce CO_2, water and heat. The liquid water generated in the cathode CL can be drained out of the cell by the capillary force and gravity, and can be vapourized to form vapour, which diffuses out of the cell. The heat generated at both the anode and cathode is rejected to the surroundings and the methanol solution in the fuel reservoir. Combining reactions (1) and (2), the overall reaction in the DMFC is

$$CH_3OH + 3/2O_2 \rightarrow CO_2 + 2H_2O + heat \qquad (3)$$
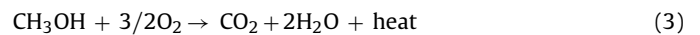
The above description reveals that during the operation of a passive DMFC, the reactants (methanol, water and oxygen) are passively supplied by diffusion and natural convection, while the products (CO_2 and water) are removed by passive forces. The unique features of such a fuel cell system are that it is both simple and compact and has no parasitic power losses. Such attributes make this type of fuel cell particularly suitable for powering portable electronic devices. Compared with relatively bulky active DMFCs, however, since the rates of passive reactant supply and product removal are much lower and more difficult to control, the passive DMFC generally generates lower output power. Hence, the most important issue in the design of the passive DMFC is how to manage the supply/removal of reactants/products without invoking any active means so that fuel cell performance can be boosted. To this end, it is essential to gain a deep insight into the critical transport issues associated with the passive supply/removal of reactants and products.

3. Critical transport issues

The passive transport mechanisms for supplying reactants and removing products described above make the mass-transport process of each species in the passive DMFC significantly different from that in active DMFCs. The critical issues related to the mass transport of different species in the passive DMFC are elaborated as follows.

3.1. Methanol transport

A critical problem with Nafion membranes used for DMFCs is that methanol, along with water, can permeate the membrane and arrive at the cathode. As mentioned earlier, methanol crossover not only leads to a decrease in cell voltage, but also wastes the fuel. Hence, the rate of methanol crossover must be minimized. As methanol crossover depends greatly on diffusion through the membrane, its rate can be significantly reduced by decreasing the methanol concentration in the anode CL. To reduce the methanol concentration for a given anode design, the methanol concentration in the fuel reservoir must be sufficiently low. On the other hand, too low a methanol concentration in the reservoir causes insufficient methanol concentration in the anode CL, resulting in a large mass-transport loss and thus a lower cell voltage. Hence, it is critical to maintain an adequate methanol concentration in the anode CL. However, it is challenging to achieve this, as the methanol concentration in the anode CL is intrinsically related to the local
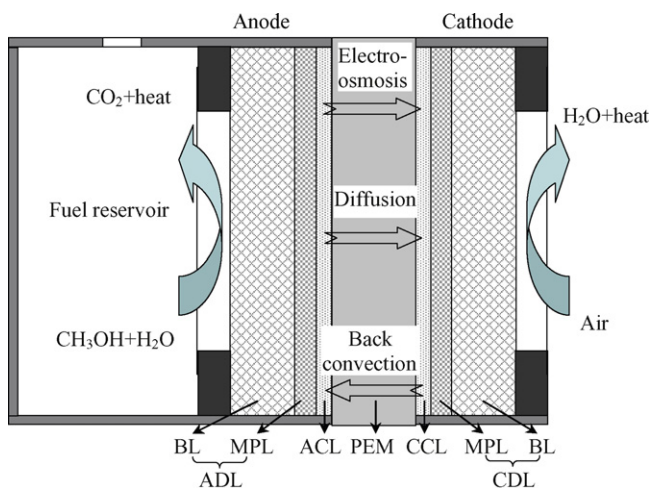

Fig. 2. Schematic of MEA and heat/mass transport in passive DMFC.

concentration of water and CO_2. A change in one of the three mass-transport processes of methanol, water and CO_2, will cause a change in the other two local concentrations in the anode CL. Hence, how to maintain passively an adequate methanol concentration in the anode CL at a given current density is a critical issue in the design of a passive DMFC.

As discussed above, constrained by the problem of methanol crossover, the methanol concentration in the fuel reservoir must be sufficiently low (2.0–4.0 M at present). This means that the specific energy of the stand-alone passive DMFC is relatively low, which results in not only a short operation time for each fuel charge, but also a quick decrease in the methanol concentration in the fuel reservoir when the cell starts discharging. The latter consequence can cause the methanol concentration in the anode CL to become insufficient, although adequate in the initial discharging period. Hence, another critical issue in the design of a passive DMFC is how to maximize the specific energy of the stand-alone system so that the operation time can be maximized and discharging can be more stable.

In summary, the main challenge regarding methanol transport in the design of a stand-alone passive DMFC is how to maximize the system-carried specified energy and simultaneously how to maintain an adequate methanol concentration in the anode CL at a given current density.

3.2. Water and oxygen transport

As there are no auxiliary fans/compressors in the passive DMFC, diffusion and natural convection are the primary transport mechanisms for delivering oxygen to the cathode CL. As a result, the oxygen mass-transport loss may become the factor that limits cell performance at high-current densities. Hence, a critical issue in the design of the passive DMFC cathode is how to minimize the oxygen mass transfer resistance from the current-collector to the cathode CL. More importantly, the mass transfer of oxygen is intrinsically related to water removal from the cathode. In active DMFCs, the liquid water at the cathode can be swept out by forced convection. In the passive DMFC, however, the water generated on the cathode, along with that passes through the membrane from the anode (termed as water crossover), can cause a more serious cathode flooding problem, as the ability to remove passively the excess water is lower than that in active DMFCs. Hence, with the constraint of passive operation, minimizing the oxygen and water transport resistances and enhancing water transport by utilizing passive forces, such as capillary action and gravity, is a critical issue in the design of the passive DMFC cathode.

In addition, as mentioned earlier, the use of Nafion membranes in DMFCs allows a significant fraction of water, which is supplied to the anode as a reactant, to be transported to the cathode. Water crossover through the membrane not only causes water loss from the anode but also exaggerates flooding at the cathode. Hence, reducing water crossover is another critical issue in the design of a passive DMFC.

3.3. Heat transport

As in other types of fuel cell, the heat generated in the electrochemical reactions in the passive DMFC also needs to be dissipated to ambient. In a fuel cell with active supply of reactants, the cell operating temperature can be regulated by the flow rates of fuel and gas and/or an added cooling fluid. In passive DMFCs, however, the cell operating temperature depends on methanol concentration (which is the only adjustable parameter) and ambient temperature. Another feature regarding heat transport in a passive DMFC is that the cathode is completely exposed to ambient, which can lead to a higher heat dissipation rate from the cell to ambient. As a result,

the operating temperature of passive DMFCs is usually low (below 35 °C) which, in turn, causes slower kinetics of the electrochemical reactions and thus lower cell performance. Therefore, how to reduce the heat loss such that the cell can operate at a sufficiently high temperature is important in the design of passive DMFCs.

4. Mass transport of methanol with low concentration

As discussed in the preceding section, it is essential to maintain an adequate methanol concentration in the anode CL at a given current density so that the rate of methanol crossover and mass-transport loss can be minimized and thus cell voltage can be maximized. Since in the passive DMFC, methanol is transported from the fuel reservoir to the anode CL by diffusion and natural convection, the methanol concentration in the anode CL is affected by many parameters, such as the methanol concentration in the fuel reservoir, the cell orientation, and the mass transfer resistance associated with a specific design, and the materials of the anode CC and DL [29,32–44]. It is important to note that an adequate methanol concentration in the anode CL can be achieved by filling a high- or a low-methanol concentration in the fuel reservoir, depending on the mass transfer resistance from the reservoir to the anode CL. If the mass transfer resistance from the fuel reservoir to the anode CL is sufficiently large, the fuel cell can be operated by using, a higher methanol concentration in the reservoir (high-methanol concentration operation). On the other hand, if no particular measures are taken to increase the mass-transfer resistance through the design of the anode CC and DL, the fuel cell can only be operated by using a lower methanol concentration in the reservoir (low-methanol concentration operation). Most of the previous work regarding the mass transport of methanol has focused on low-methanol concentration operation. The discussion about the effects of different parameters on the mass transport of methanol in this section is confined to low-methanol concentration operation (<5.0 M), while the case with high-methanol concentration operation is discussed later in Section 5.

4.1. Effect of methanol concentration

For a given design of a passive DMFC and cell orientation, the methanol concentration in the fuel reservoir is the only parameter that can be varied to achieve an adequate methanol concentration in the anode CL. Hence, the effect of this parameter on passive DMFC performance has been the subject of many studies [29,32–37]. Park et al. [29,32,33] and Kim et al. [34] showed that a methanol concentration of 4.0 M gave the best cell performance and the improved performance with increasing the methanol concentration from 1.0 to 4.0 M was attributed to the improved mass transfer of methanol from the fuel reservoir to the anode CL. Liu et al. [37] later revisited the effect of methanol concentration on the performance of a passive DMFC and their results are presented in Fig. 3. The data show that both the limiting current density and the peak power density exhibit a tremendous increase when the methanol concentration is raised from 1.0 to 2.0 M. When the methanol concentration was increased from 2.0 to 5.0 M, the cell performance kept improving, but the increments became progressively smaller toward the highest methanol concentration. A maximum power density of 20 mW cm^{-2} was obtained with a 5.0 M methanol solution. The increase in cell performance with increasing methanol concentration can be attributed to the increased mass-transfer rate of methanol, as evidenced from the increased limiting current from the 1.0 to the 2.0 M operation. More importantly, they found that the cell operating temperature also increased with increasing methanol concentration. As shown in Fig. 4, cells fed with lower methanol concentrations (1.0 and 2.0 M) are virtually operated at
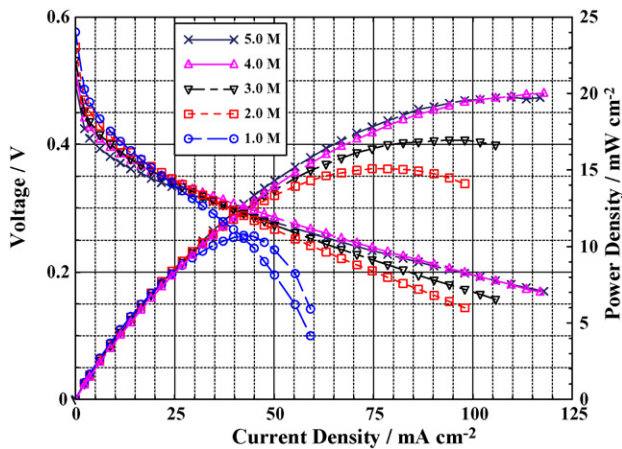
Fig. 3. Effect of methanol concentration on performance of passive DMFC [37].

a temperature close to room temperature (22–23 °C). With 4.0 and 5.0 M methanol concentrations, however, the operating temperature rose to 32 and 36.5 °C, respectively. A higher methanol concentration leads to a higher rate of methanol crossover from the anode to the cathode. The exothermic reaction between the permeated methanol and oxygen on the cathode generates more heat with a higher methanol concentration and thereby results in a higher operating temperature. As a result, a higher temperature will lead to higher electrochemical kinetics of methanol oxidation and oxygen reduction reactions. Moreover, the internal resistance of the cell decreases with increasing temperature, which also improves cell performance. More recently, Guo and Faghri [38] investigated the effect of methanol concentration on the performance of a passive DMFC and they also found the correlation between the methanol concentration and cell operating temperature.

In summary, for a given design of a passive DMFC, increasing the methanol concentration in the fuel reservoir from lower to higher values can lead to an increase in the mass-transfer rate of methanol from the fuel reservoir to the anode CL, thus improving cell performance. When the methanol concentration is too high, however, the rate of methanol crossover will be high and thereby increase the mixed potential on the cathode and, in turn, decrease the cell voltage. More importantly, it should be recognized that in passive DMFCs, the cell operating temperature is inherently coupled with the methanol concentration. This is a feature of a passive DMFC that distinguishes it from an active DMFC, in which the cell operating
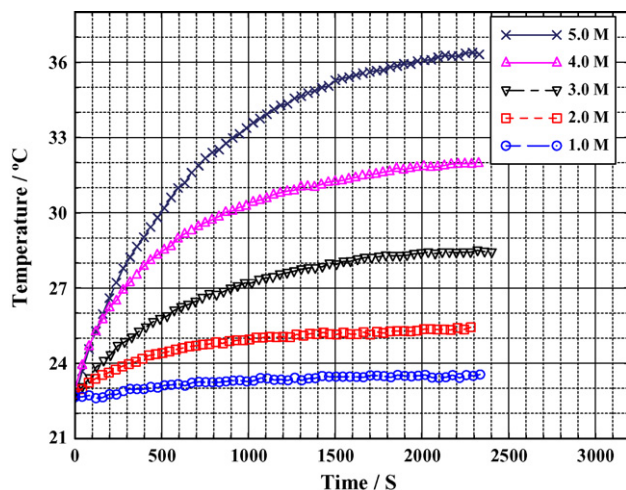

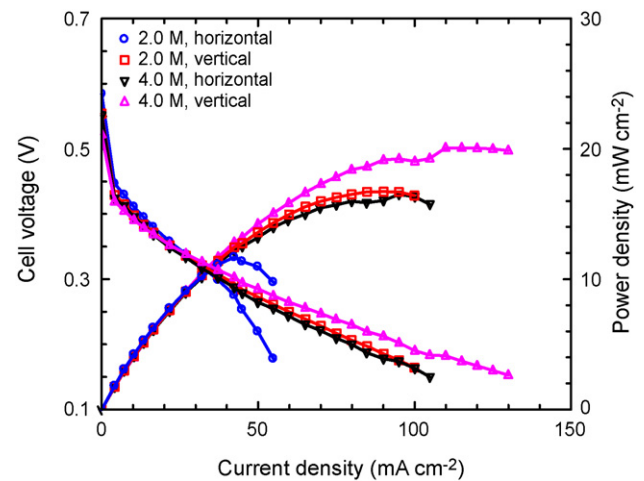Fig. 4. Variation in cell operating temperature [37].

temperature can be regulated by varying the flow rates of fuel and oxygen/air. Hence, cautions need to be taken given that changing the methanol concentration in the fuel reservoir of a passive DMFC also means changing its operating temperature.

4.2. Effect of cell orientation

On the anode of a passive DMFC, the methanol transport is affected by natural convection due to the density difference between the liquid phase and CO_2. Also, on the anode, the temperature decreases from the electrode toward the fuel reservoir, which can enhance natural convection on the anode. In addition, on the cathode, there exists a temperature difference between the electrode and ambient air that causes the air near the electrode to rise naturally. Since the strength of natural convection depends on the orientation, the cell orientation of the passive DMFC affects not only the methanol transport at the anode, but also oxygen and water transport at the cathode.

Chen et al. [39] investigated the effect of cell orientation on the performance of a passive DMFC. The fuel cell was tested with (i) a vertical orientation (as shown in Figs. 1 and 2), (ii) a horizontal orientation with the anode facing upward, and (iii) a horizontal orientation with the anode facing downward. For case (iii), it was found that the generated CO_2 bubbles accumulated on the upper surface of the anode CC, blocking the methanol transport and eventually ceasing the fuel cell operation. The results for cases (i) and (ii) are presented in Fig. 5. It is found that the vertical orientation yields better performance than the horizontal orientation at middle and high-current densities. At low-current densities, however, the performance of the horizontal cell is superior. The lower voltages at low-current densities with the vertical orientation may be attributed to a higher rate of methanol crossover, which is due to the fact that natural convection is stronger than in the horizontal cell. On the other hand, a higher rate of methanol crossover can result in a higher cell operating temperature in the vertical cell, as shown in Fig. 6, as more heat can be generated from the exothermic reaction between the permeated methanol and oxygen on the cathode. The increased temperature accelerates both the methanol oxidation and oxygen reduction reactions, and thus the vertical orientation yields the higher voltages at middle and high-current densities. Moreover, a lowered internal cell resistance at the higher cell operating temperature may also improve cell performance. It should be noted that the increased cell operating temperature can also enhance the transport of water and oxygen as a result of enhanced natural convection
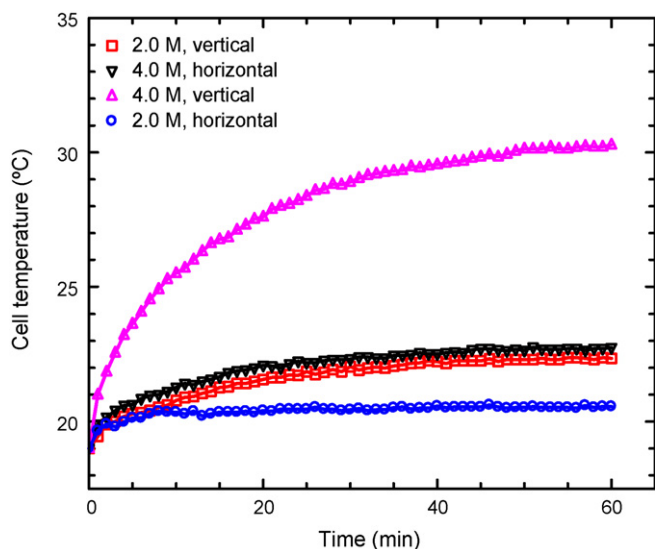

Fig. 5. Effect of cell orientation on performance of passive DMFC with different methanol solutions [39].

Fig. 6. Variation in cell operating temperature with different cell orientations [39].

Fig. 8. Comparison in cell operating temperatures with active oxygen feed among different cell orientations at 2.0 M operation [39].

with the vertical orientation, which also enhances cell performance.

To verify whether the improved cell performance of the vertical cell is mainly due to increased kinetics of the methanol oxidation and oxygen reduction reactions or to enhanced natural convection at the cathode, Chen et al. [39] tested a passive DMFC with an active supply of oxygen while keeping a passive supply of methanol at the anode. The results are presented in Fig. 7 and show that, under the condition of the active oxygen supply, the performance of the vertical cell is still higher than that of the horizontal cell. This is because the operating temperature of the vertical cell is higher, as shown in Fig. 8. This finding indicates that the improved performance of the vertical cell is mainly attributed to the increased kinetics of the methanol oxidation and oxygen reduction reactions as a result of the increased temperature, although oxygen transport is also enhanced. More recently, Lai et al. [40] also investigated the effect of the cell orientation on the performance of a passive DMFC and found that the vertical orientation yielded better performance.

In summary, for a given cell design and methanol concentration, vertical operation can increase the mass-transfer rate of methanol from the fuel reservoir to the anode CL because of the stronger natural convection at this orientation. As a result, the rate of methanol
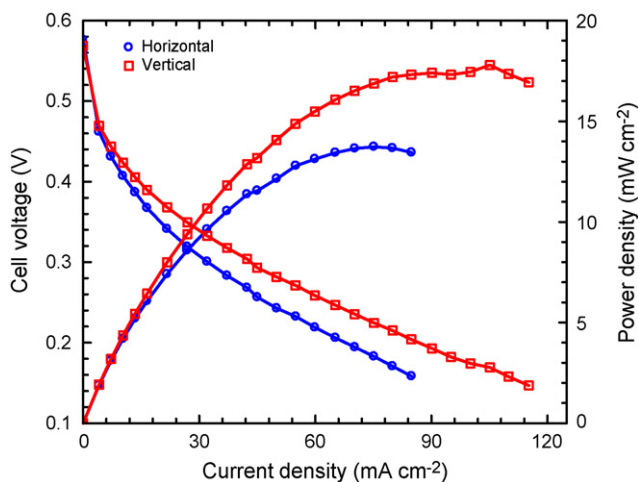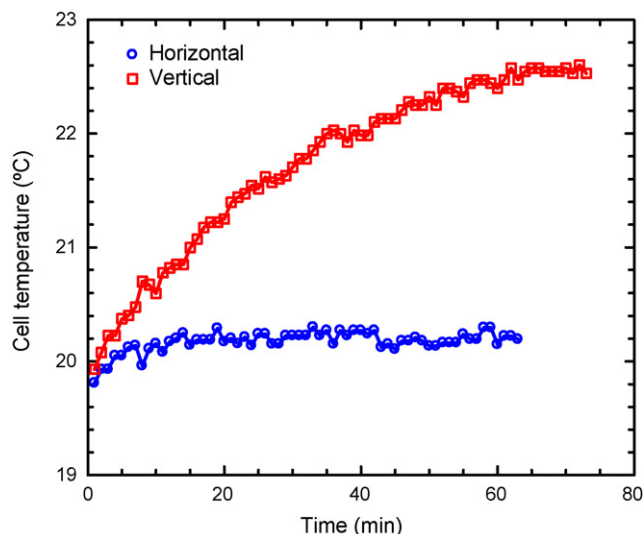
crossover in the vertical cell is higher than in the horizontal cell, which leads to a higher operating temperature, and thus faster kinetics of the methanol oxidation and oxygen reduction reactions and higher voltages at high-current densities.

4.3. Effect of anode current-collector

As a key component in the passive DMFC, the anode current-collector (CC) not only collects the current from the anode DL but also provides passages for transporting methanol, water and CO_2. Two typical designs of the anode CC for passive DMFCs, namely, perforated and parallel current-collectors, are illustrated in Fig. 9. Yang et al. [41] compared these two designs with low-methanol concentration operation and found that the perforated current-collector yielded lower performance, which was attributed to the following two reasons. First, since the open ratio of the perforated current-collector was much lower than that of the parallel current-collector, the mass-transfer resistance of methanol was higher with the former. As a result, for the same methanol concentration in the reservoir, the increased mass-transfer resistance with the perforated current-collector resulted in an insufficient methanol concentration in the anode CL, which increased the mass-transport loss at the anode and thus lowered the cell voltage. Second, gas bubbles are prone to block part of the holes of the perforated current-collector, further increasing the mass-transfer resistance of methanol with the perforated current-collector. It is important to note that a high-mass-transfer resistance through the anode CC and DL is not a problem, as an adequate methanol concentration can be achieved by increasing the methanol concentration in the fuel reservoir. In addition, current-collectors made of metal foam [42] and mesh [38,43] have also been tested in passive DMFCs. Guo and Faghri [38] compared different metal-mesh current-collectors with different thicknesses; each current-collector was either put directly on the anode DL or hot-pressed on the anode DL. It was found that the cell with the thicker current-collector that was hot-pressed showed the highest performance as a result of the lowest contact resistance between the anode CC and DL.

In summary, as part of the entire methanol transport path from the fuel reservoir to the anode CL, the design of the anode CC has a significant impact on the performance of passive DMFCs that are operated with low-methanol concentration. It must be noted, however, that for a given anode CC design, an adequate methanol concentration in the anode CL can be achieved by adjusting the

Fig. 7. Comparison in cell performance with active oxygen feed among different cell orientations at 2.0 M operation [39].

methanol concentration in the fuel reservoir and the design of the anode DL. To increase the system specific energy, an anode CC with a higher mass-transfer resistance of methanol is desired. In addition, the electrical contact resistance between the anode CC and DL has to be minimized in the design of an anode CC.

4.4. Effect of anode diffusion layer

The anode diffusion layer (DL) usually consists of two layers, a backing layer (BL) that is made of carbon cloth or carbon paper, and a microporous layer (MPL) that is composed of hydrophobic polymer and carbon powder. The function of the anode DL is to conduct current from the anode CL to the anode CC and to distribute methanol over the anode CL. Hence, the standard to judge whether the design of the anode DL is good or bad is to see whether it has a higher electrical conductivity and whether it can make methanol more evenly distributed over the anode CL. Instead of using carbon paper and cloth, Liu et al. [33] used a sintered stainless-steel fibre felt as the anode BL for a passive DMFC and found that it yielded better cell performance, mainly because the metal DL had higher electrical conductivity than does the carbon paper. Kim et al. [44] developed an anode MPL consisting of nano-sized silica particles and a binder that was coated on the anode BL made of a carbon

paper from SGL®. They found that, due to its hydrophilicity, this new design could facilitate a more even distribution of methanol in the anode CL and effective mass transport of methanol and water, and an effective removal of CO_2. These reported studies indicate that the methanol transport from the fuel reservoir to the anode CL and the reverse CO_2 transport are also affected by the properties of the anode DL. An anode DL with hydrophilic surfaces can enhance both CO_2 removal and methanol transport. Note that the enhancement of mass transport becomes necessary only if the methanol concentration in the fuel reservoir is low. Similar to the design of the anode CC, however, an anode DL with a higher mass-transfer resistance is necessary to achieve an increase in specific energy. In addition, an anode DL with high-electrical conductivity is also required to reduce the internal cell resistance for improving cell performance.

In summary, the mass transport of methanol in a passive DMFC is influenced by the material properties and design parameters of the anode DL and CC as well as by operating conditions such as methanol concentration and cell orientation. To achieve better performance, it is essential to maintain an adequate methanol concentration in the anode CL at a given current density so that both the rate of methanol crossover and the mass-transport loss at the anode is minimized. In the meantime, it should be noted that as the cell operating temperature is intrinsically coupled with the methanol concentration in the anode CL, the change in temperature due to the change in methanol concentration in the anode CL can more significantly affect the cell performance. In terms of electronic transport, the anode CC and DL should be made of materials that have high-electrical conductivity. More importantly, it is important to recognize that anode CCs and DLs with higher mass-transfer resistance of methanol are desired so that the specific energy of the fuel cell system can be increased, as discussed in the next section.
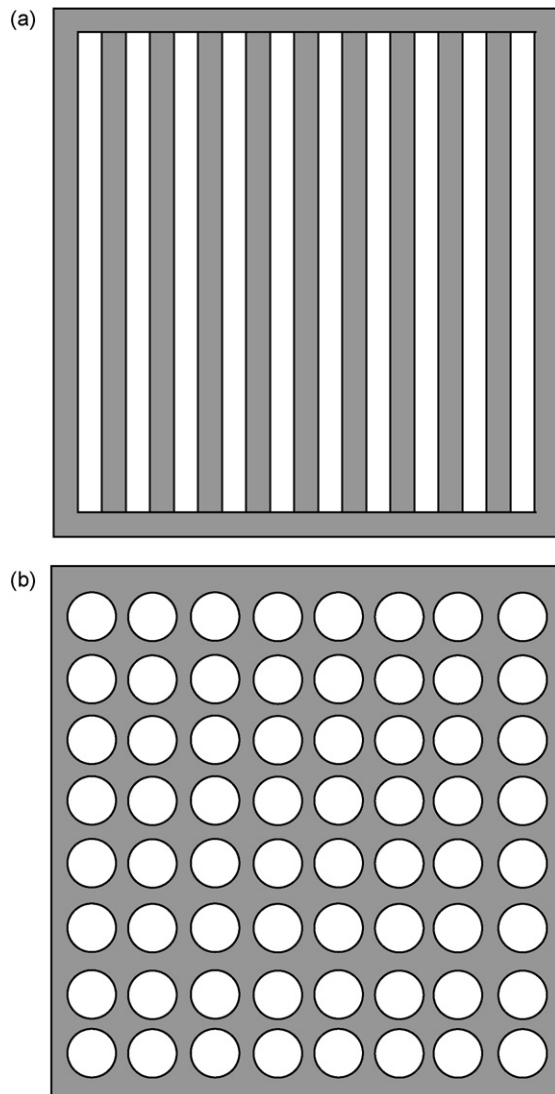
5. Mass transport of methanol with high concentration

Due to the problem of methanol crossover, most of the previous work has focused on studying passive DMFCs with low-methanol concentrations in the fuel reservoir (<5.0 M), as discussed in the preceding section. Filling the fuel reservoir with a low-methanol concentration means that the specific energy of the fuel cell system is low, which not only leads to a short operation time for each fuel charge, but also results in a rapid decrease in the pre-set methanol concentration in the fuel reservoir. Hence, filling in the fuel reservoir with a high-methanol concentration is desired. This can be achieved by increasing the mass-transport resistance of methanol from the fuel reservoir to the anode CL [45–52] so that an adequate methanol concentration can be maintained.

Abdelkareem et al. [45–47] added a dense porous carbon plate between the fuel reservoir and the anode CC of a passive DMFC; the results of performance tests are given in Fig. 10. The data show that the added mass-transfer resistance of methanol resulting from the porous carbon plate makes it possible for the passive DMFC to be operated with high-methanol concentration. For example, a 16-M methanol solution at room temperature yields a maximum power density of 24 mW cm^{-2}. Zhang and Hsing [48] developed an integrated anode CC and DL made of a single flexible graphite plate. The high-mass-transfer resistance through this graphite plate allowed a DMFC to be operated with 12-M methanol concentration. Kim et al. [49,50] added hydrogels to the fuel reservoir to reduce the rate of methanol transport from the fuel reservoir to the anode CL so that the passive DMFC can operate at high-methanol concentration. Similarly, Pan [51] and Oedegaard et al. [52] employed a Nafion-based permeable material as a barrier layer to resist methanol transport to the anode CL.
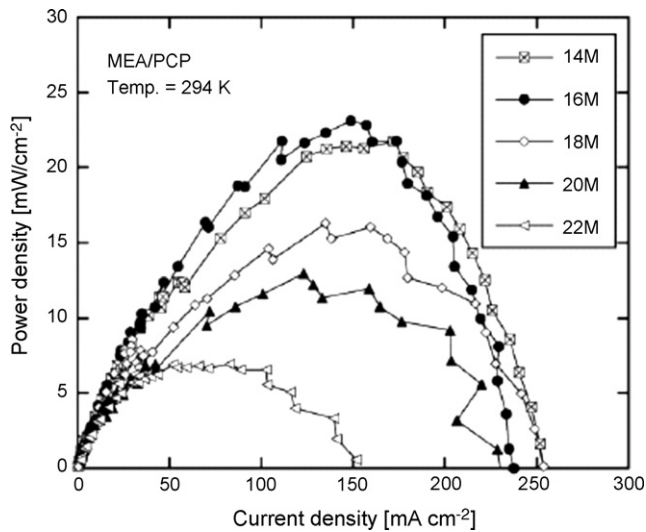

Fig. 9. Different current-collectors for passive DMFCs: (a) parallel current-collector; (b) perforated current-collector.

Fig. 10. Performance of passive DMFC with porous plate, MEA/PCP, within high-methanol concentration range from 14 M to neat methanol [46].

In summary, increasing the mass-transfer resistance of methanol from the fuel reservoir to the anode CL enables a passive DMFC to be operated at high-methanol concentration while maintaining an adequate methanol concentration in the anode CL so that the specific energy of the system can be maximized. In addition, the increased methanol concentration in the fuel reservoir as a result of the increased mass-transfer resistance of methanol can also slow down the decrease in the methanol concentration in the fuel reservoir due to the consumption, and thereby results in more stable discharging.

6. High-concentration methanol supply system

The mass transport of methanol in passive DMFCs with a relatively simple methanol supply system (as shown in Figs. 1 and 2) in which methanol solution is interfaced with a current-collector-clamped MEA has been discussed in Sections 4 and 5. It has been concluded that operation with a high-methanol concentration can be achieved by increasing the mass-transfer resistance of methanol from the reservoir to the anode CL. This section is still concerned with high-methanol concentration operation, but the idea is to modify the conventional fuel supply system without adding any methanol transport barrier before the MEA [53–56]. For instance, Guo and Faghri [54] developed a fuel storage and supply system, in which methanol and water are stored in two separated containers. These two containers are then routed to a porous structure that is interacted with the anode CC. During operation, the stored methanol and water are transported to the porous structure, mainly by diffusion. A pre-set low-methanol concentration in the porous structure can be formed by controlling the respective flow rates of methanol and water transport from the methanol and water containers. Since the design of this fuel supply sub-system can allow the fuel cell to carry pure methanol while maintaining an adequate methanol concentration in the anode CL, the system specific energy can be high.

More recently, Chan et al. [56] proposed a self-regulated passive fuel-feed system driven by the exhausted CO_2 for use in a passive DMFC. This passive fuel-feed system is shown schematically in Fig. 11, which consists of a reaction chamber, a fuel tank with a built-in spring, a fuel feed valve, and a pressure-release valve. During operation, a highly concentrated methanol solution stored in the fuel tank is supplied to the anode reaction chamber in response to the methanol consumption rate, while the methanol concentration
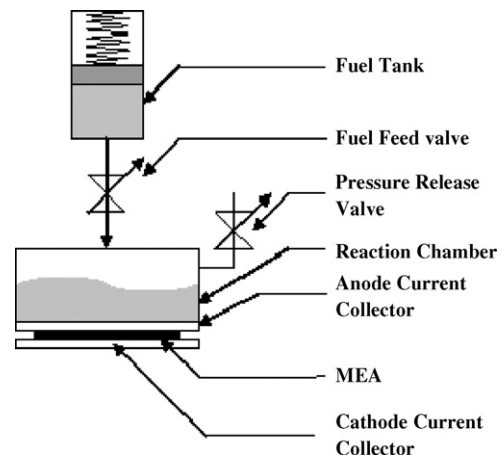

Fig. 11. Schematic of passive DMFC with passive fuel-feed system [56].

in the anode reaction chamber is maintained at an adequate value to minimize the rate of methanol crossover and mass-transport loss. The feeding rate from the fuel tank to the reaction chamber is controlled by the CO_2 generation rate, which is proportional to current density and is automatically regulated by the gas pressure inside the reaction chamber. The working principle of this fuel-feed system is outlined in Fig. 12. When the fuel cell is discharged, the generated CO_2 flows to the sealed reaction chamber such that the pressure increases with time. Once the pressure reaches a certain value P_1, both the feed valve and the pressure-release valve are opened. Subsequently, the high-methanol concentration solution stored in the fuel tank is fed to the reaction chamber driven by a spring, while the accumulated CO_2 in the reaction chamber is released to the ambient, causing a decrease in the reaction chamber pressure. When the pressure decreases to a sufficiently low value, both valves are closed and CO_2 starts to build-up the pressure inside the reaction chamber again, thereby forming a working cycle. If the discharging current is decreased, less methanol will be consumed by the electrochemical reaction and thus the resulting CO_2 generation rate is reduced. This leads to a slower increase in the pressure inside the reaction chamber. The working cycle becomes longer, and results in a lower feeding rate such that the passive fuel-feed system can self-regulate the feeding rate in response to a change in the dis-
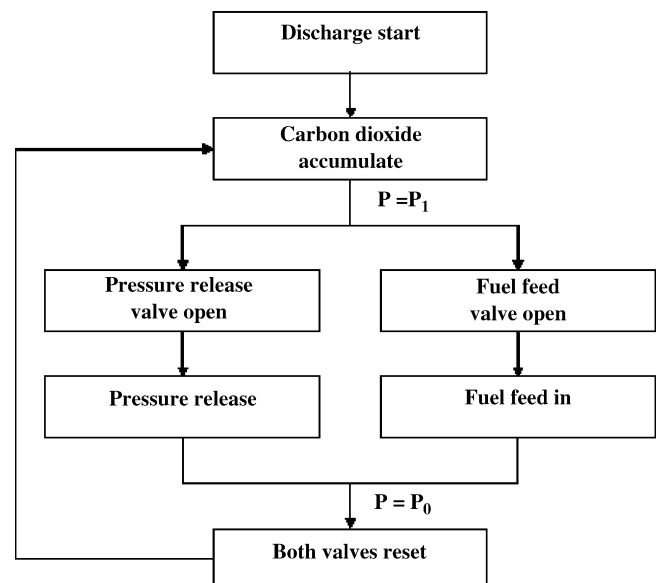

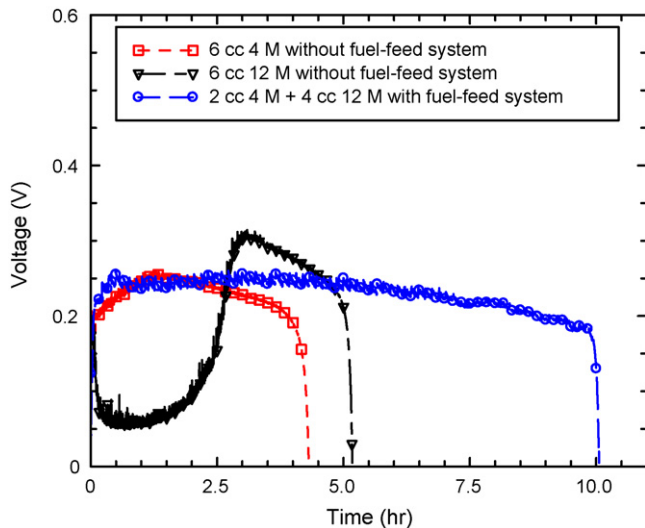**Fig. 12.** Operation flow chart of passive fuel-feed system [56].

Fig. 13. Performance curve for DMFCs with and without passive fuel-feed system operated at current density of 50 mA cm^{-2} [56].

Fig. 14. Vapourized methanol delivery system with utilization of heat generated by fuel cell [58].

charging current. Meanwhile, since this passive fuel supply system allows a highly concentrated methanol solution to be supplied to a passive DMFC, the specific energy of the stand-alone system is high and hence operation time can be long.

The performance of passive DMFCs with and without the fuel-feed system and with 4.0- and 12.0-M methanol solutions for a given current density of 50 mA cm^{-2} are shown in Fig. 13, which shows that the cell with the fuel-feed system yielded a stable and almost the same cell voltage as that of a conventional cell at 4.0-M operation. This implies that although the 12.0-M methanol is supplied to the fuel cell system, the methanol concentration in the reaction chamber is still maintained at the adequate value with the help of the fuel-feed system so as to produce the same voltage as the 4.0-M operation. More importantly, the cell with this fuel supply system exhibits a much longer operation time (10.1 h) than does the conventional design (4.4 h) as a result of the increased specific energy of the stand-alone system. In addition, the authors also compared the cell performance with that of the conventional design at 12.0-M operation and found that the cell voltage and operation time are much lower because of severe methanol crossover in the conventional design. To demonstrate that the new fuel-feed system can self-regulate the methanol feed rate in response to the discharging current density, Chan et al. [56] also discharged the fuel cell at a current density of 30 mA cm^{-2} and found that the system could successfully operate at a stable cell voltage for 14.5 h.

Another approach to increase the specific energy is to supply pure liquid methanol and vapourize it before being fed to the fuel cell. In such an approach with pure methanol but no water supply, the water required by the methanol oxidation reaction on the anode can be internally transferred from the cathode. An important feature of this approach is that an adequate methanol concentration in the anode CL can be readily achieved by adjusting the methanol evaporation rate. Kim [57] introduced a multi-layered porous structure consisting of a Nafion 112 membrane, a barrier and a buffer layer on the anode of a passive DMFC. The supplied liquid methanol vapourizes as a result of a reduction in pressure after passing through the membrane. Both the barrier and buffer reduce the methanol concentration to the desired value in the anode CL. Guo and Faghri [58] proposed generation of methanol vapour by utilizing the heat produced by the fuel cell itself; the idea is illustrated in Fig. 14. The liquid methanol is introduced from the fuel tank to a porous pad, where it vapourizes as a result of heating from a heat spreader that conducts the heat from the MEA. Recently, Eccarius et
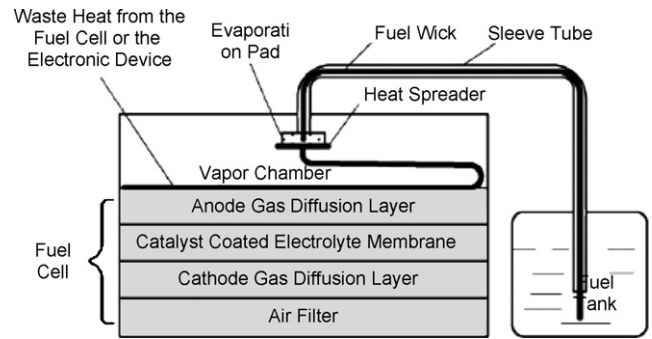
al. [59] developed a fuel supply system, in which a phase-separation membrane was used to generate methanol vapour. They found that in such a pure methanol supply system, transporting water from the cathode was a critical issue.

In summary, the above-mentioned fuel supply systems can be effective in maximizing the system specific energy while maintaining an adequate methanol concentration in the anode CL. When supplying pure methanol with no water, it should be recognized that transporting water from the cathode to the anode for the methanol oxidation reaction is critical to sustain the operation of passive DMFCs. Water transport through the MEA is discussed in the next section.

7. Water and oxygen transport

In the passive DMFC, oxygen is transported from ambient air to the cathode CL by diffusion and natural convection, while the removal of water generated at the cathode, along with that crosses from the anode, relies on passive forces, such as capillary and gravitational forces. Such a passive operation may result in more serious cathode water flooding, resisting the oxygen transport. Therefore, enhancing water and oxygen transport under passive operating conditions is the key to boost the performance of passive DMFCs. To this end, it is essential to gain a better understanding of how the design parameters of the MEA and current-collector design, as well as operating conditions, affect water and oxygen transport in passive DMFCs [39,40,44,60–69].

7.1. Effect of MEA design

The MEA design, particularly the cathode DL that consists of a backing layer (BL) and a microporous layer (MPL), plays an important role in water and oxygen transport. Since water crossover through the membrane can intensify cathode water flooding, efforts have been devoted to the optimization of the MEA design to reduce water crossover or to transport water from the cathode to the anode. The basic idea is to build up a hydraulic liquid pressure in the cathode with a highly hydrophobic cathode MPL. Peled et al. [60,61] added a hydrophobic water barrier layer in the cathode of a passive DMFC and showed that varying the thickness and material of the barrier layer allowed the rate of water crossover to vary from negative, through zero, to positive values. With such a water barrier layer, it is possible to make a passive DMFC operate under water-neutral conditions. It has also been shown that a double-layered hydrophobic MPL with different compositions [44] and a double-layered highly hydrophobic cathode BL with an added air filter [62] allowed a reduction in water crossover. It should be noted that a highly hydrophobic cathode DL not only can reduce water crossover but also tends to reduce the liquid water saturation in the cathode DL, which fur-
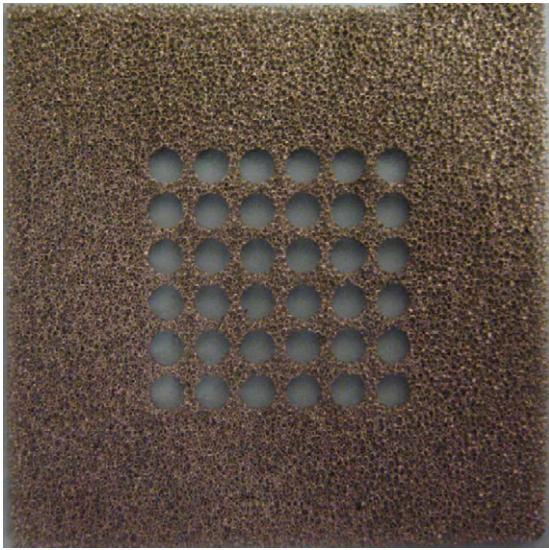
Fig. 15. Schematic of porous current-collectors [67].

Fig. 17. Variation in cell operating temperature with different cathode current-collectors [67].

ther mitigates cathode water flooding and thus enhances oxygen transport.

Recently, the effect of membrane thickness on water crossover in passive DMFCs was investigated. Jewett et al. [62] found that thicker membranes exhibited greater water balance coefficients, higher fuel utilization efficiency, and greater energy efficiency. By contrast, Song et al. [63] found that water crossover could be lowered by using thinner membranes. This discrepancy among different researchers may be due to the competition between the back-convection flux from the cathode to the anode and the diffusion flux from the anode to the cathode.

In addition to water transport, the MEA design also affects oxygen transport in passive DMFCs and thus the cell performance. Reshetenko et al. [65] applied pore-forming materials, such as ammonium carbonate and ammonium hydrocarbonate, to the cathode CL to form mesopores so that the rate of oxygen transport, as well as the electrochemical active area and catalyst utilization, can be increased; they found that the power density was increased by 30–40% with adding the pore-forming materials. Reshetenko et al. [66] also optimized the structure of the cathode CL for air-breathing DMFCs by using carbon nanotubes (CNTs) as an pore-forming additive. It was demonstrated that the porosity of the cathode CL was increased as a result of the morphology of CNTs. This, in turn, caused
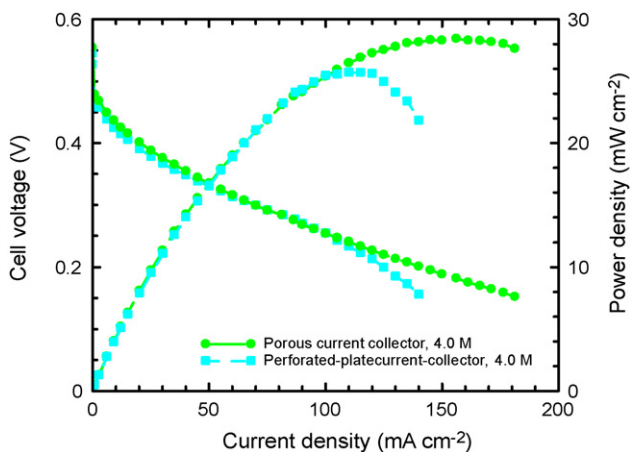
an increase in the oxygen transfer rate and thereby improved cell performance.

7.2. Effect of cathode current-collector

The purpose of the cathode current-collector is not only to collect the electric current and but also to offer passages for oxygen and water transport. Yang et al. [41] studied the effect of current-collector structure on the performance of a passive DMFC; their results showed that a parallel current-collector was better than a perforated current-collector in terms of water removal from the cathode. One disadvantage of the perforated and parallel current-collectors is that their ribs tend to accumulate liquid water and reduce the cathode area to be exposed to ambient air. To overcome this disadvantage, Chen and Zhao [67] recently proposed a porous current-collector made of metal foam, as shown in Fig. 15, to replace conventional perforated and parallel current-collectors. The performance of passive DMFCs with porous and perforated current-collectors under 4.0-M methanol concentration operation are compared in Fig. 16. The results show that, at low-current

Fig. 16. Comparison in cell performance between different cathode current-collectors [67].
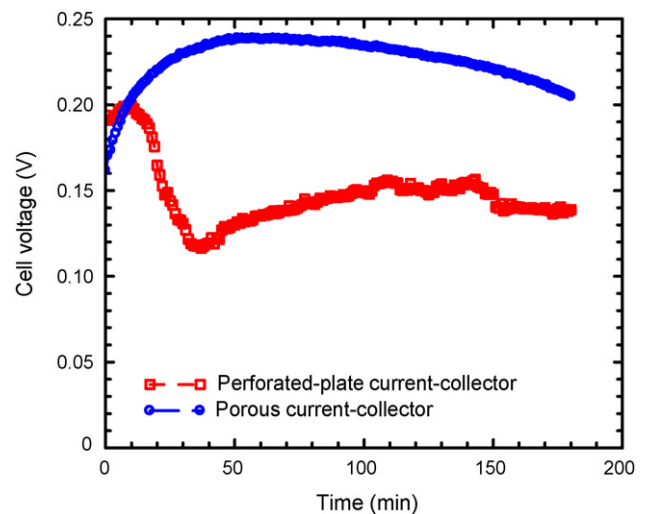

Fig. 18. Transient discharging voltage at constant-current density (80 mA cm^{-2}) with start from cell to be fuelled with methanol solutions between different cathode current-collectors [67].

densities, the porous current-collector yields higher voltages than the perforated current-collector, while at middle current densities, the cell voltages of both the current-collectors are almost the same. Interestingly, at high-current densities, the porous current-collector exhibits much higher voltages than the perforated current-collector. The improved performance with the porous current-collector at low- and high-current densities is attributed to the following two reasons. First, the overall mass-transfer resistance of oxygen through the porous current-collector is lower than that with the perforated current-collector as a result of the larger specific mass-transfer area, which enhances oxygen transport and thus increases the cell voltages. Second, the lower effective thermal conductivity of the porous current-collector yields a higher cell operating temperature, as shown in Fig. 17, and further improves the cell performance. At middle current densities, however the increased cell voltages as a result of the increased mass-transfer rate of oxygen and cell operating temperature is compensated by the higher internal cell resistance of the cell with the porous current-collector. Therefore, the voltages at middle current densities are almost the same with either current-collector. Furthermore, the enhanced oxygen transport was confirmed by the electrochemical impedance spectra (EIS) measurement for passive DMFCs with porous and perforated current-collectors.

Chen and Zhao [67] also investigated the long-term performance of passive DMFCs with both cathode current-collectors. The results, shown in Fig. 18, reveal that although the porous current-collector exhibits a lower voltage as a result of the higher internal cell resistance in the initial period, after 15 min, the voltage of the cell with porous current-collector is higher than that with the perforated current-collector as a result of the larger specific mass-transfer area and the faster water removal rate due to the capillary action in such a porous structure.

The use of a porous metal current-collector also makes it possible to eliminate the cathode DL so that the single porous metal foam layer serves not only to collect current but also to transport water and oxygen [68]. The new design is shown in Fig. 19(b), as compared with the conventional design shown in Fig. 19(a). The new design enables lower overall mass-transfer resistances of oxygen and water that can be elucidated as follow. The cathode overpotential for the conventional design can be expressed by

$$\eta_c = \frac{RT}{\alpha F} \ln \left(\frac{(i + i_p)C_{O_2}^{ref}}{i_{O_2}^{ref}(C_{O_2}^{\infty} - ((i + i_p)/4F)((1/h) + (l_{cc}/D_{O_2,cc}^{eff}) + (l_{dl}/D_{O_2,dl}^{eff})))} \right) \quad (4)$$

which indicates that the cathode overpotential η_c decreases with decreasing the mass-transfer resistance in each layer, including $1/h$ at the cathode current-collector surface, $l_{dl}/D_{O_2,dl}^{eff}$ in the cathode DL, and $l_{cc}/D_{O_2,cc}^{eff}$ in the cathode CC. As a consequence, if the cathode DL can be removed, the overall mass-transfer resistance of oxygen can be reduced, thereby increasing the cathode potential. Hence, the new design illustrated in Fig. 19(b), which combines the cathode DL and current-collector into a single layer, can result in a lower mass-transfer resistance of water and oxygen. The IR-corrected performance of passive DMFCs with the conventional and the new design under 4.0-M methanol concentration operation is compared in Fig. 20. The data show that the new MEA exhibits higher voltages than the conventional MEA as a result of the lowered overall mass-transfer resistance of oxygen. The increment becomes larger with increasing current density as a result of the increased demand of oxygen at the cathode. Fig. 21 shows the transient voltages at a constant current density for the new and conventional MEAs. It is clear that the new MEA yields substantially higher voltages due to the higher rates of oxygen transport and water removal that result from the lower overall mass-transfer resistance.
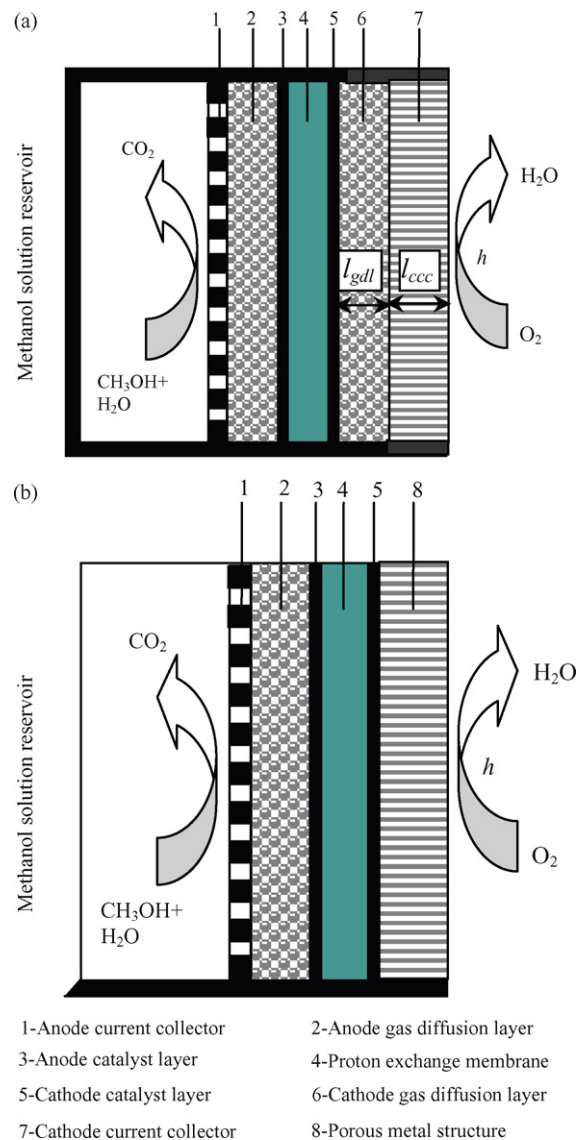

1-Anode current collector   2-Anode gas diffusion layer
3-Anode catalyst layer   4-Proton exchange membrane
5-Cathode catalyst layer   6-Cathode gas diffusion layer
7-Cathode current collector   8-Porous metal structure

Fig. 19. Schematic of passive DMFC with (a) conventional MEA and (b) new MEA [68].
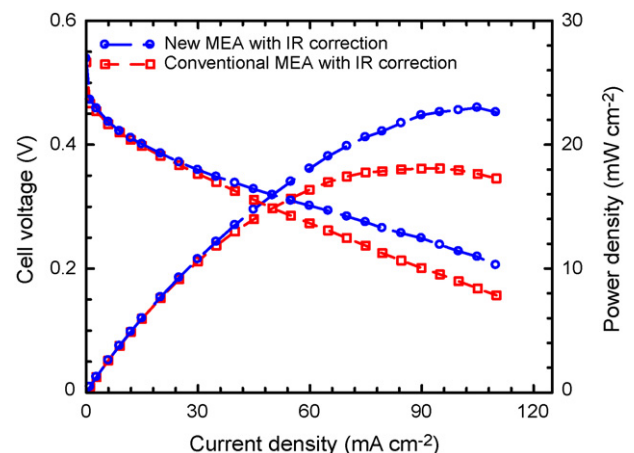

Fig. 20. Comparison in cell performance between new and conventional MEAs [68].
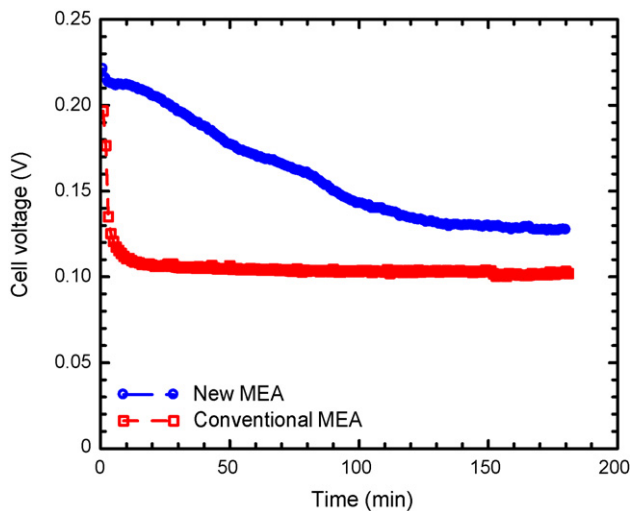
Fig. 21. Transient discharging voltage at a constant-current density ($50\,mA\,cm^{-2}$) with start from cell to be fuelled with methanol solutions between new and conventional MEAs [68].

7.3. Effect of operating conditions

The operating conditions that affect water and oxygen transport in a passive DMFC include cell orientation and current density [39,40,69]. Fig. 22 compares the long-term operation of a passive DMFC at different orientations [39]. Although the vertical orientation generally shows higher voltages than the horizontal orientation with the anode facing upward as a result of the higher cell operating temperature, the horizontal orientation with the anode facing upward yields much more stable voltages due to the higher rate of liquid water removal at the cathode with the aid of gravity. It should be pointed out that a passive DMFC in a horizontal orientation with the anode facing downward will result in extremely unstable operation, as the removal of CO_2 bubbles from the anode and the removal of water from the cathode become rather difficult. Lai et al. [40] investigated a passive DMFC at different currents with different cell orientations and draw a similar conclusion that a passive DMFC with the anode facing upward showed the best long-term discharge performance at high current because of the enhanced water removal by gravity. Chen and Yang [69] found that
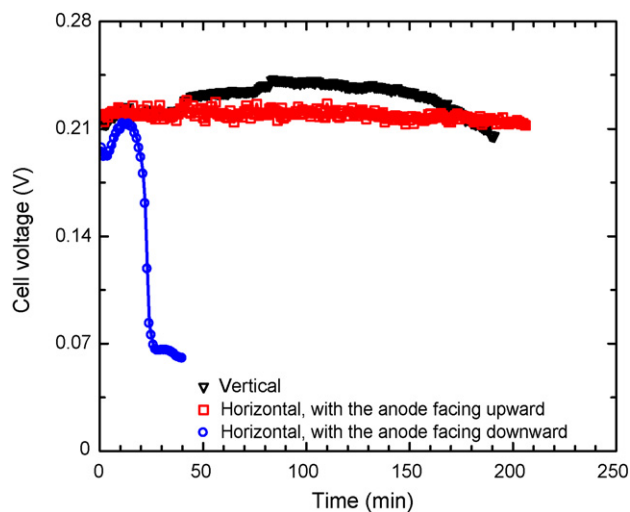

Fig. 22. Transient discharging voltage at constant current density ($60\,mA\,cm^{-2}$) with start from cell to be fuelled with 4.0 M methanol solutions at different cell orientations [39].

the discharge current has a strong impact on the operation stability of a passive DMFC; a high-discharge current may lead to more serious cathode flooding, because of the higher water generation rate, and therefore, more unstable voltages.

The above discussion indicates that the water and oxygen transport in passive DMFCs is influenced by the MEA and current-collector design, as well as by the operating conditions. The key to achieve higher cathode potential is to enhance oxygen and water transport by better utilization of passive forces such as capillary and gravitational forces. It is also important to optimize the MEA design to reduce water crossover across the membrane so that water flooding at the cathode can be mitigated.

8. Heat transport

In a passive DMFC, the heat generated from the electrochemical reactions is mainly transported to the anode fuel reservoir and the cathode ambient air. To maximize oxygen transport, the cathode of a passive DMFC is usually completely exposed to ambient air. This, however, also maximizes the rate of heat dissipation from the cell to ambient. As a result, the cell operating temperature of passive DMFCs is usually low, resulting in poor kinetics of the electrochemical reactions. Hence, efforts [54,67] have been made to the study of reducing heat dissipation from the cathode to increase the cell operating temperature. For instance, Guo and Faghri [54] added an air filter with low-thermal conductivity at the cathode of a passive DMFC so that the heat dissipation from the cathode was reduced, due to the increased heat-transfer resistance, and the cell operating temperature increased. The added air filter could also increase the mass-transfer resistance of water vapour, leading to a higher concentration of water vapour in the cathode. The increased water vapour concentration may reduce the liquid water evaporation at the cathode, further increasing the cell operating temperature. Therefore, the cell performance of the passive DMFC with an added air filter is improved as a result of the increased cell operating temperature. It should be noted, however, that the added air filter can also increase the mass-transfer resistances of oxygen from the ambient air to the cathode CL and liquid water removal from the cathode CL to ambient. Accordingly, the oxygen concentration in the cathode CL is decreased and the cathode voltage is lowered. It should be mentioned that the earlier-discussed porous current-collector made of metal foam [67] not only can offer a smaller mass-transfer resistance of water and oxygen, but also can reduce the heat dissipation from the cathode due to the lower effective thermal conductivity of the porous structure.

In summary, the conventional design of passive DMFCs results in a high rate of heat dissipation from the cell to the fuel reservoir and to ambient air. As a result, the cell operating temperature is usually low. It is therefore essential to reduce the heat dissipation so that the fuel cell can be operated at a sufficiently high temperature.

9. Passive DMFC stack

To fulfill the power requirement of a specific application, a fuel cell stack, in which unit cells are connected in series or in parallel, is needed. In general, high-current output can be obtained by increasing the MEA area, whereas high-voltage output can be achieved by increasing the number of unit cells that are connected in series. Most stacks are in-series connections. According to the arrangement of unit cells, in-series stacks can be classified into two types: a bipolar stack and a monopolar stack. Usually, passive DMFC stacks [22,25,33,34,38,69–76] adopt the monopolar arrangement as this arrangement can make the air-breathing cathode completely exposed to ambient air to maximize oxygen and water transport.
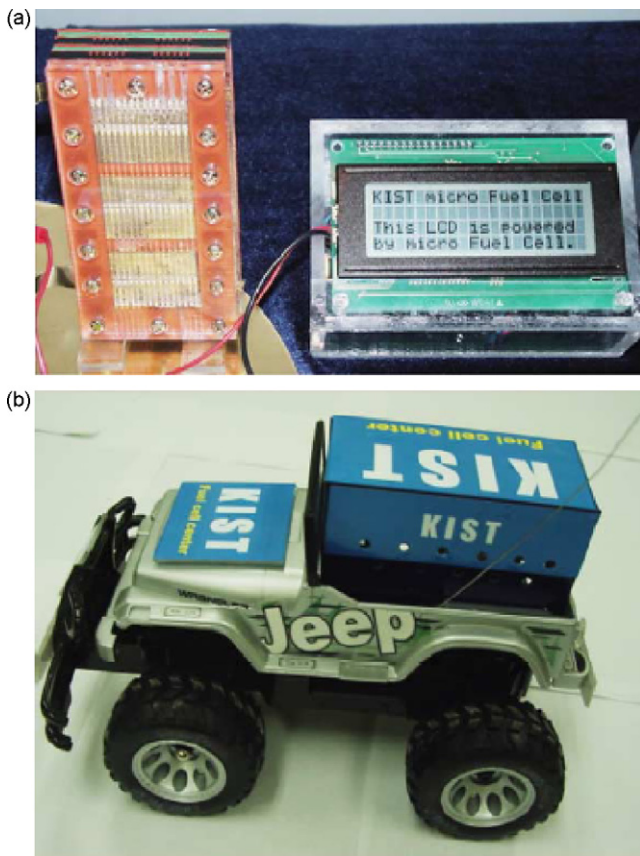
Fig. 23. (a) LCD panel and (b) toy car powered by micro-DMFC stacks made at KIST [34].

Fig. 24. Effect of methanol concentration on performance of passive DMFC stack [76].

Chang et al. [22] designed and fabricated a passive DMFC stack with 12 unit cells, each of which had an active area of 2.0 cm², connected in series. This passive DMFC stack provided a peak power output of 560 mW at 2.8 V. Liu et al. [33] developed a passive DMFC stack consisting of 12 unit cells to power a mobile phone; a stack with 2.0-M methanol solution provided around 3.7 V during both the talk and standby modes. Chen et al. [25,69] also developed a passive DMFC stack of four unit cells to supply power for a continuously operating mobile phone in talk mode via a dc–dc converter. With this stack, the mobile phone could sustain 50 min of talk for each fuel charge. To demonstrate the feasibility as a portable-power source, Kim et al. [34] designed and fabricated a passive DMFC stack to power a LCD panel and a toy car, as shown in Fig. 23; the developed stack could provide a power of 1.0 W and a power density of 37 mW cm⁻². Recently, Guo and Faghri [38] developed a passive DMFC stack with a window-frame cell fixture to hold the current-collector and MEA together, providing an even distribution of compressive force for the fuel cells; additionally, the stack design is modular and thereby allows the fuel cell components to be fabricated separately. Using this stack design, Guo and Faghri [71] further developed a 1-W passive DMFC with a passive ancillary system, which utilized porous media for fuel storage and delivery and for water management. More recently, Cao et al. [72] designed, fabricated and tested silicon-based micro-DMFC stacks that consisted of six unit cells; the results showed that a stack with double serpentine-type flow-fields generated a peak power of 151 mW at a voltage of 1.5 V.

The effects of various design parameters and operating conditions on stack performance have also been investigated [73,74]. Kim et al. [73] developed a passive DMFC stack of six unit cells and investigated the in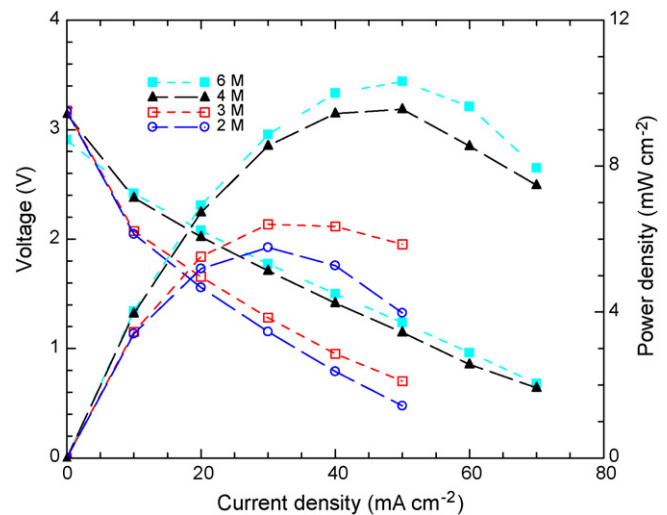fluence of operating conditions such as the cell temperature and methanol concentration on stack performance. It was found that with increasing methanol concentration: (i) the open-circuit voltage (OCV) decreased as a result of the higher rate of methanol crossover; (ii) the cell operating temperature increased and caused an improvement in cell performance. Baglio et al. [74] investigated the effect of MEA design and operating conditions on a passive DMFC stack, including the catalyst loading and methanol concentration; they found that the stack with an unsupported Pt loading of 4.0 mg cm⁻² gave the best performance at 5.0 M operation.

Recently, Chan et al. [76] designed, fabricated and tested a small passive DMFC stack and investigated the effect of methanol concentration on stack performance and the effect of cell operating temperature on water flooding; the results are presented in Fig. 24. The performance of the stack increases with increasing methanol concentration as a result of the increased cell operating temperature caused by the exothermic reaction between the permeated methanol and oxygen at the cathode. This is in agreement with the results reported for the single cell [37]. On the other hand, the increased operating temperature reduced water flooding at the air-breathing cathode on account of the increased water evaporation rate, which further increased the cell voltage and operation stability. It was also found that with the same methanol concentration, the stack exhibited a much higher cell operating temperature (50–53 °C) than the unit cell (27–29 °C), which tends to increase the performance.

In summary, to maximize water and oxygen transport to the air-breathing cathode, the monopolar arrangement is widely used in formation of passive DMFC stacks. The stack performance is affected by many design parameters and operating conditions, including methanol concentration, catalyst loading, MEA and current-collector design. All the key issues to boost single-cell performance also apply for the passive DMFC stack, including maintaining an adequate methanol concentration and sufficiently high temperature, as well as enhancing water and oxygen transport at the cathode.

10. Modelling of passive DMFCs

As the intrinsically coupled physicochemical processes occur simultaneously in passive DMFCs, including two-phase heat and mass transfer, electrochemical reactions, as well as ionic and electronic transfer, it is difficult to quantify experimentally the
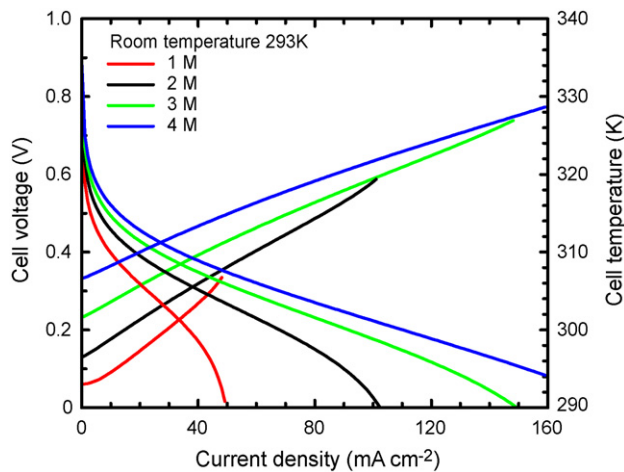
Fig. 25. Polarization curves of passive DMFC and cell temperature at cathode catalyst layer operating with different methanol concentrations [79].

Fig. 26. Polarization curves for 4 M methanol operation with and without operating temperature lowered to value of 2 M methanol operation under OCV condition [79].

interrelated parameters that govern the fuel cell. Therefore, numerical modelling that incorporates coupled two-phase heat and mass transport and electrochemical kinetics becomes essential to gain a better understanding of passive DMFCs and to shorten the design and optimization cycles.

Mathematical models for passive DMFCs are generally developed based on single-phase or two-phase mass transport. Hwang et al. [77] developed a single-phase, three-dimensional, numerical model to evaluate an air-breathing cathode of a DMFC. This model simulated the diffusive transport of different gas species in the cathode DL using the Stefan–Maxwell equation, the electrochemical reaction in the cathode CL using the Butler–Volmer equation, and the charge transport in the porous electrode using Ohm's law. With this model, the effect of the air-breathing hole size of the cathode current-collector was investigated and optimized. Yeh and Chen [78] developed a single-phase, one-dimensional, numerical model that incorporated the mixed potential effect as a result of methanol crossover on a passive DMFC. With this model, they investigated the impacts of the anode and cathode catalyst layers, membrane thickness, membrane conductivity and methanol concentration on cell performance.

The above-mentioned examples of single-phase mass-transport models did not consider the temperature gradient in the fuel cell structure. Recently, however, Chen and Zhao [79] developed a one-dimensional, single-phase, mass-transport model with the heat transfer effect taken account. With this model, they investigated the effect of methanol concentration on the performance of a passive DMFC. The polarization curves with 1.0–4.0 M methanol solution operations are given in Fig. 25 and show that, with an increase in methanol concentration, the cell performance upgrades progressively. This result is qualitatively in agreement with the experimental data discussed earlier [37]. The increased cell performance at higher methanol concentration is not only because a higher methanol concentration in the fuel reservoir reduces the mass-transport loss with low-methanol concentrations, but also because the increased rate of methanol crossover due to the higher methanol concentration leads to a higher heat generation, which in turn increases the cell operating temperature, as also shown in Fig. 25. The increased cell operating temperature accelerates the electrochemical reactions of both methanol oxidation and oxygen reduction, thereby increasing the cell voltage. In order to prove that the increased temperature is more important in terms of performance enhancement than the improved mass transport of methanol with a higher methanol concentration, the numerical results for 4.0-M operation without control of temperature and
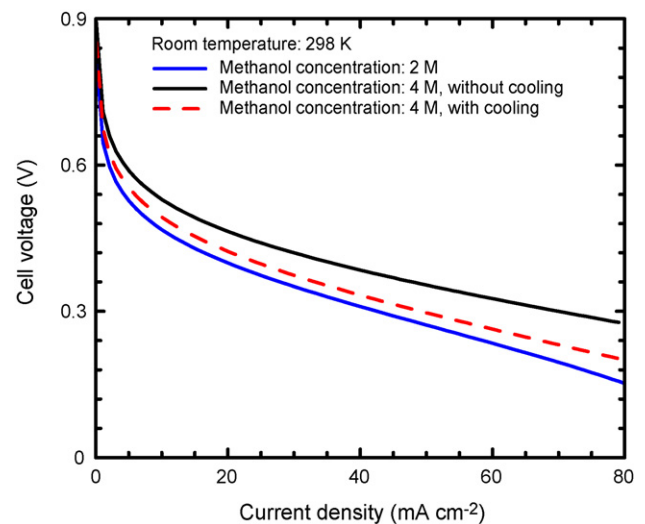
the same concentration but with the temperature lowered to the same as that of the 2.0-M operation are obtained and presented in Fig. 26. It is clear that the increased cell voltage as a result of increasing methanol concentration is lowered when the temperature is substantially lowered, indicating that the improved performance of a passive DMFC running with higher methanol concentrations is attributed primarily to the higher cell operating temperature caused by the exothermic reaction between the permeated methanol and oxygen on the cathode.

It should be noted that single-phase models are limited to low-current densities. At high-current densities, the increase in gas bubbles at the anode of the fuel cell demands a more realistic two-phase heat and mass-transport model. Recently, Rice and Faghri [80–82] developed a multi-phase, multi-component model for a passive DMFC with a passive methanol delivery system consisting of a porous structure; the effects of the methanol concentration and the properties of porous medium used for the passive methanol delivery system on cell performance were explored. Faghri et al. [83] also developed a numerical model to simulate a vapourized passive DMFC; with this model, the vapour methanol transport and two-phase water transport were studied and the numerical results revealed that the water supply to the anode for methanol oxidation reaction is critical for successful operation of this type of fuel cell.
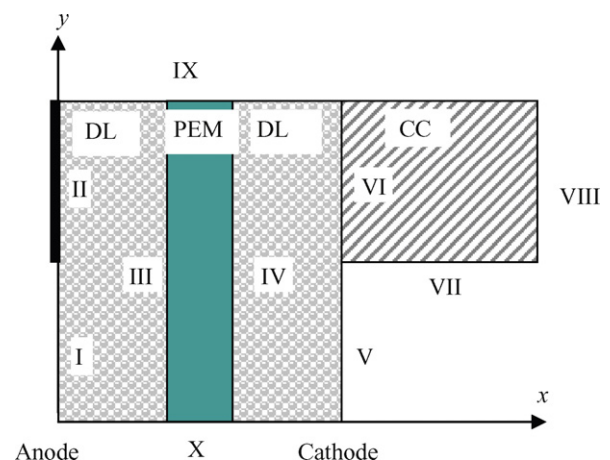

Fig. 27. Schematic of computation domain [84].

Table 1
Constitutive relations and definitions [84].

Parameters	Expressions
Capillary pressure	$p_c = p_g - p_l = \sigma \cos\theta_c (\varepsilon/K)^{0.5} J(s)$ $$J(s) = \begin{cases} 1.417(1-s) - 2.120(1-s)^2 + 1.263(1-s)^3 & 0° < \theta_c < 90° \\ 1.417s - 2.120s^2 + 1.263s^3 & 90° < \theta_c < 180° \end{cases}$$
Relative permeability	$k_{rl} = s^3$ (liquid) $k_{rg} = (1-s)^3$ (gas)
Effective diffusion coefficients of species	$D_i^{\text{eff}} = D_i \varepsilon^{1.5}(1-s)^{1.5}, \quad i : O_2,$ vapor (CGDL) $D_i^{\text{eff}} = D_i \varepsilon^{1.5} s^{1.5}, \quad i :$ methanol (AGDL)
The saturation pressure of vapour	$\log_{10} p_v^{\text{sat}} = -2.1794 + 0.02953(T-273) - 9.1837 \times 10^{-5}(T-273)^2 + 1.4454 \times 10^{-7}(T-273)^3$ atm
Interfacial transfer rate of water between liquid and vapour	$$R_w = \begin{cases} k_e \dfrac{\varepsilon s \rho_l}{M_{H_2O}}(y_v p_g - p_v^{\text{sat}}) & y_v p_g < p_v^{\text{sat}} \\ k_v \dfrac{\varepsilon(1-s)y_v}{RT}(y_v p_g - p_v^{\text{sat}}) & y_v p_g > p_v^{\text{sat}} \end{cases}$$

More recently, Chen et al. [84] developed a two-dimensional, two-phase, thermal model for a passive DMFC with the computation domain illustrated in Fig. 27. In the horizontal direction, the anode CC and fuel reservoir is not included as these components are assumed to be well insulated from the ambient and the methanol concentration in the fuel reservoir is assumed to be constant during the fuel cell discharging process. In the vertical direction, only the half-channel and half-rib width are included because of the lateral symmetry with respect to the middle point of channel width. For convenience of description, each boundary and interface are designated with Roman numerals from I to X. The mass transport of liquid and gas phases in the anode DL can be modelled by

$$\nabla \cdot (D_m^{\text{eff}} \nabla C_m^{\text{adl}}) = 0 \quad \text{(liquid phase)} \tag{5}$$

and

$$\nabla \cdot \left(\frac{\rho_g}{M_g} \frac{K k_{rg}}{\mu_g} \sigma \cos(\theta_c) \left(\frac{\varepsilon}{K} \right)^{0.5} \nabla J(s) \right) = 0 \quad \text{(gas phase)} \tag{6}$$

where D_m^{eff}, ρ_g, M_g, K, k_{rg} and μ_g represent the effective diffusivity of methanol in the anode DL, the density and molar weight of gas CO_2, the absolute permeability of the anode DL, the relative permeability and viscosity of the gas phase, respectively. $J(s)$ represents the Levertte function with s being the liquid saturation in a porous medium (see Table 1).

The mass transport of O_2, water vapour, and liquid water in the cathode DL can be modelled by

$$-\nabla \cdot (-D_{O_2}^{\text{eff}} \nabla C_{O_2}^{\text{cdl}}) = 0 \quad \text{(gas phase)} \tag{7}$$

$$-\nabla \cdot (-D_v^{\text{eff}} \nabla C_v^{\text{cdl}}) - R_w = 0 \quad \text{(gas phase)} \tag{8}$$

and

$$\nabla \cdot \left(-\frac{\rho_l}{M_l} \frac{K k_{rl}}{\mu_l} \sigma \cos(\theta_c) \left(\frac{\varepsilon}{K} \right)^{0.5} \nabla J(s) \right) + R_w = 0 \quad \text{(liquid phase)} \tag{9}$$

where $D_{O_2}^{\text{eff}}$, D_v^{eff}, ρ_l, M_l, k_{rl}, μ_l, p_l and R_w stand for the effective diffusivities of the oxygen and water vapour, the density and molar weight of the water, the relative permeability and viscosity and pressure of the liquid phase, and the interfacial transfer rate of water between liquid and water vapour, respectively.

The flux of methanol through the membrane, N_{cross}, can be determined from

$$N_{\text{cross}} = -D_{m,\text{mem}}^{\text{eff}} \frac{dC_{m,\text{mem}}}{dx} + n_d^m \frac{i}{F} \tag{10}$$

where $D_{m,\text{mem}}^{\text{eff}}$ is the effective diffusivity of methanol in the membrane, F is the Faraday's constant ($96,485\,\text{C mol}^{-1}$), n_d^m is the electro-osmotic drag coefficient of methanol. The transport of liquid water through the membrane is assumed to be driven by the electro-osmotic drag, and thus the flux of water can be determined by considering the electro-osmotic drag only, i.e.

$$N_{H_2O} = n_{H_2O} \frac{i}{F} \tag{11}$$

with n_{H_2O} denoting the electro-osmotic drag coefficient of water.

The heat generated by the electrochemical reaction in the anode CL is given by

$$q_{\text{acl}} = i \left(\eta_a - \frac{\Delta H_a - \Delta G_a}{6F} \right) \tag{12}$$

where the first term represents the heat generation due to the activation and mass-transfer overpotentials on the anode; the second term represents the entropy change of the anodic electrochemical reaction with ΔH_a denoting the anodic reaction enthalpy and ΔG_a the Gibbs free energy.

The heat generation in the cathode CL, q_{ccl}, can be determined from

$$q_{\text{ccl}} = (i + i_p)\eta_c - (i + i_p) \frac{\Delta H_c - \Delta G_c}{4F} - i_p \frac{\Delta H_a - \Delta G_a}{6F} \tag{13}$$

where the first term represents the heat generation due to activation and mass-transfer overpotentials and the mixed potential caused by methanol crossover on the cathode; the second term accounts for the entropic loss with ΔH_c denoting the cathodic reaction enthalpy and ΔG_c the Gibbs free energy.

Assuming that convection is small, the heat-transfer process through the membrane, cathode DL and CC can be modelled by

$$\nabla \cdot (-\lambda_i \nabla T) = 0, \quad i : \text{MEM}, \text{ CC} \tag{14}$$

Table 2
Boundary conditions [84].

	Boundary conditions
I	$C_m = C_{m,\infty}, s = 0.95$
II	$\frac{dC_m}{dx} = 0, \quad \frac{ds}{dx} = 0$
III	$N_m = \frac{i}{6F} + N_{\text{cross}}, \quad -\frac{K\rho_g k_{rg}}{M_g \mu_g} \nabla p_g = \frac{i}{6F}, \quad q_{\text{acl}} = i \left(\eta_a - \frac{\Delta H_a - \Delta G_a}{nF} \right)$
IV	$N_{O_2} = \frac{i}{4F} + \frac{3}{2} N_{\text{cross}}, \quad N_{H_2O} = 2N_{\text{cross}} + n_{H_2O} \frac{i}{F} + \frac{i}{2F}, \quad q_{\text{ccl}} = (i + i_p)\eta_c - i \frac{\Delta H_c - \Delta G_c}{nF}$
V	$C_{O_2} = C_{O_2,\infty}, \quad C_v = C_{v,\infty}, \quad s = 0.05, \quad -\lambda_{\text{cgdl}} \frac{dT}{dx} = h(T - T_\infty)$
VI	$\frac{dC_{O_2}}{dx} = 0, \quad \frac{dC_v}{dx} = 0, \quad \frac{ds}{dx} = 0, \quad \lambda_{\text{cgdl}} \frac{dT}{dx} = \lambda_{\text{ccc}} \frac{dT}{dx}$
VII	$\lambda_{\text{ccc}} \frac{dT}{dy} = h(T - T_\infty)$
VIII	$-\lambda_{\text{ccc}} \frac{dT}{dx} = h(T - T_\infty)$
IX	$\frac{dC_m}{dy} = 0, \quad \frac{dC_{O_2}}{dy} = 0, \quad \frac{dC_v}{dy} = 0, \quad \frac{ds}{dy} = 0, \quad \frac{dT}{dy} = 0$
X	$\frac{dC_m}{dy} = 0, \quad \frac{dC_{O_2}}{dy} = 0, \quad \frac{dC_v}{dy} = 0, \quad \frac{ds}{dy} = 0, \quad \frac{dT}{dy} = 0$

and

$$\nabla \cdot (-\lambda_i \nabla T) = h_v R_w, \quad i : \text{DL} \qquad (15)$$

where λ_i is the effective thermal conductivity of each component; h_v is the latent heat of vapourization of liquid water; R_w is the water evaporation rate.

The current density can be determined by the simplified Tafel equation with accounting for the effect of gas void fraction in the anode CL for a given anode overpotential:

$$i = i_m^{\text{ref}} \frac{C_{m,\text{acl}} s}{C_m^{\text{ref}}} \exp\left(\frac{\alpha_a F}{RT_{\text{acl}}} \eta_a\right) \qquad (16)$$

where i_m^{ref}, C_m^{ref}, $C_{m,\text{acl}}$ represent, respectively, the reference exchange current density on the anode, the reference concentration of methanol and the methanol concentration in the anode CL.

On the cathode, to account for the effect of methanol crossover, it is assumed that the permeated methanol from the anode completely reacts electrochemically with oxygen to form the internal current i_p. Based on this assumption, the internal current due to the methanol oxidation on the cathode can be obtained:

$$i_p = \frac{1}{6F} N_{\text{cross}} \qquad (17)$$

As a result, the cathode overpotential, taking account of the methanol crossover and liquid water saturation, can be determined

from

$$i + i_p = i_{O_2}^{\text{ref}} \frac{C_{O_2,\text{ccl}}(1-s)}{C_{O_2}^{\text{ref}}} \exp\left(\frac{\alpha_c F}{RT_{\text{ccl}}} \eta_c\right) \qquad (18)$$

where $i_{O_2}^{\text{ref}}$, $C_{O_2}^{\text{ref}}$ and $C_{O_2,\text{ccl}}$ represent, respectively, the reference exchange current density on the cathode, the reference concentration of oxygen and the oxygen concentration in the cathode CL. To solve these governing equations, the boundary conditions at each interface shown in Fig. 27 are given and detailed in Table 2.

With this model, the effects of the various operating and geometric design parameters on species distribution, current density distribution and temperature distribution, as well as the cell performance, can be studied. Fig. 28(a) shows the effect of methanol concentration on the performance of a passive DMFC; the numerical results show that the cell performance increases with the methanol concentration as a result of the increased mass-transfer rate of methanol at the anode and also the increased cell operating temperature shown in Fig. 28(b). These results qualitatively agree with both the experimental data and one-dimensional single-phase model results discussed earlier [37,79]. Fig. 29(a) presents the effect of the open ratio on the cell performance of the passive DMFC; the numerical results show that the cell performance increases with the open ratio. The improved performance with the larger open ratio can be primarily attributed to the enhanced mass-transfer
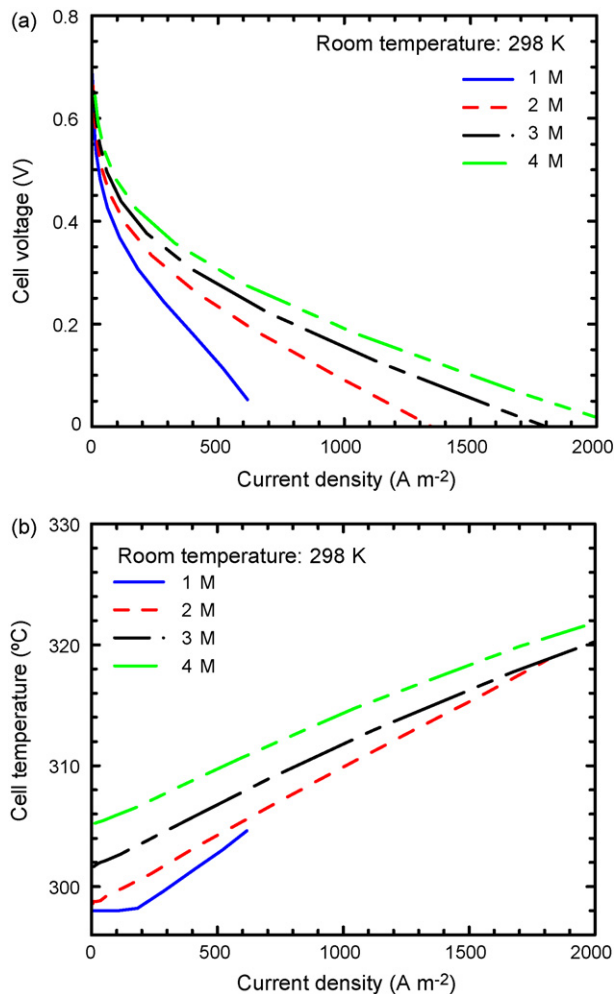

Fig. 28. Effect of methanol concentration on: (a) passive DMFC performance; (b) cell operating temperature with current density [84].
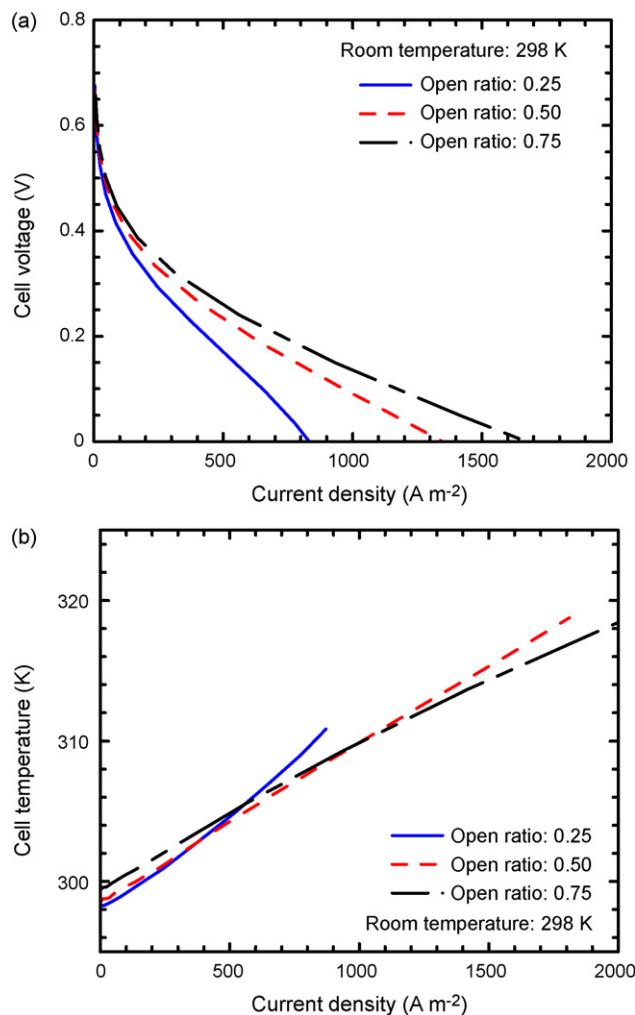

Fig. 29. Effect of open ratio on: (a) passive DMFC performance; (b) cell operating temperature with current density [84].
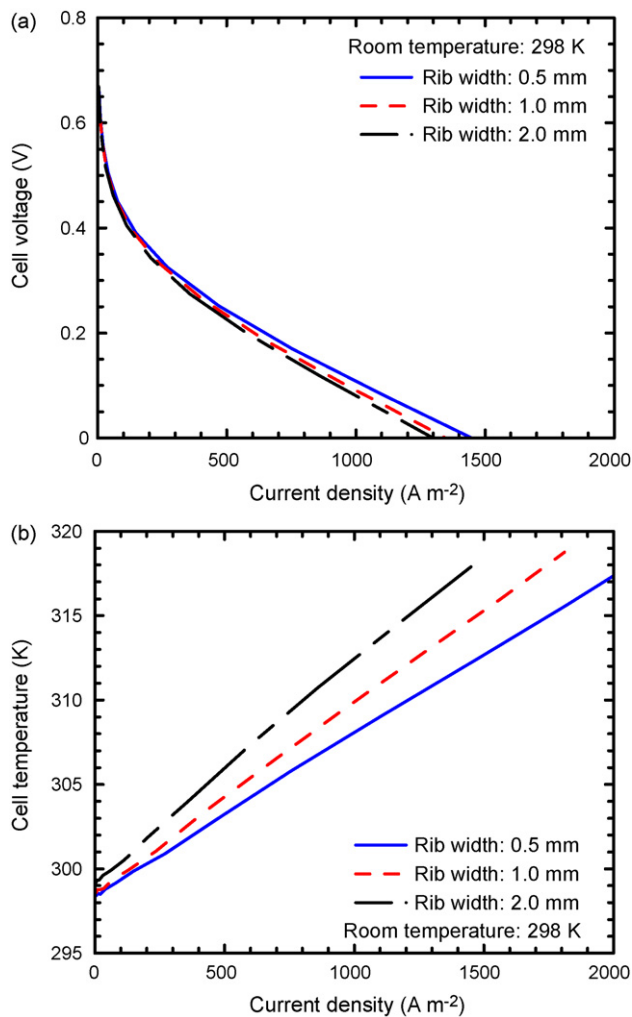
Fig. 30. Effect of channel and rib width on: (a) passive DMFC performance; (b) cell operating temperature with current density [84].

rates of both methanol and oxygen, leading to increased methanol and oxygen concentrations in both the anode and cathode CLs and thereby lowering mass-transport losses. The corresponding variation in the cell operating temperature at the anode CL with the current density for different open ratios are also obtained and presented in Fig. 29(b). The data show that, at low-current densities, the larger open ratio yields a slightly higher cell operating temperature than does the smaller one. This is because the larger open ratio exhibits a higher rate of methanol crossover and the heat generation rate caused by the methanol crossover is dominant at low-current densities, whereas at high-current densities the trend reverses because the smaller open ratio shows a higher mass-transport loss and the heat generation rate caused by mass-transport loss predominates. The effect of the channel and rib width on the performance of a passive DMFC and the cell operating temperature are shown in Fig. 30. Although the cell temperature is higher with the larger rib width operation, the cell performance is still lower, indicating that the mass transfer is a predominant factor that affects the cell performance when the rib width is varied.

The above mathematical models of the passive DMFC indicate that the performance of a passive DMFC is influenced by the cell design and operating conditions. More importantly, it is further revealed that the cell operating temperature is intrinsically coupled with the methanol concentration; the change in temperature due to the change in methanol concentration can significantly affect the cell performance. Moreover, to obtain a deep understanding of the coupled two-phase heat and mass transport in the passive DMFCs, two-phase mass-transport modelling with consideration of the thermal effect is needed.

11. Concluding remarks

The mass-transport mechanisms of reactants and products in passive DMFCs that have no liquid pumps and gas blowers/compressors are different from those in active DMFCs. Such a passive supply of the reactants and removal of the products result in many challenging issues, which affect the fuel cell performance. This review has given a comprehensive review of past experimental and numerical studies of heat and mass transport in passive DMFCs. Emphasis is placed on the mechanisms and the key issues of mass transport of each species through the fuel cell structure under the influence of passive forces, including mass transport of methanol, a passive fuel supply system with high concentration, water and oxygen transport, and heat transport. The past investigations have laid a solid foundation for the basic understanding of how the design of different MEA components and current-collectors, as well as the operating conditions, affect cell performance, operating stability, and system specific energy. Future research of mass and heat transport in passive DMFCs should be directed to addressing the following critical issues.

1. For mass transport at the anode, increasing the fuel feed concentration but maintaining an adequate concentration in the anode CL at a given current density is the direction to maximize the system specific energy and cell performance. This goal can be achieved by an optimum design of the fuel supply system, the anode current-collector, and the anode diffusion layer. In addition, it is also essential to design a fuel supply system that allows the orientation-independent operation of the fuel cell.
2. For the oxygen transport at the cathode, the key issue is how to enhance the oxygen supply to the cathode catalyst layer and the removal of water from the cathode diffusion layer by utilizing passive forces, such as the capillary action and gravity.
3. The direction of water management in passive DMFCs is to transport the water produced on the cathode through the membrane to the anode to compensate the water required in the anode methanol oxidation reaction so that the fuel cell can be operated with pure methanol and with minimum flooding at the cathode. This can be achieved by innovation in the design of the membrane electrode assembly.
4. The key issue with regard to heat transport in a passive DMFC is the proper selection of materials and the design of the cell structure so that the heat dissipation from the cell can be minimized, and the fuel cell can operate at a sufficiently high temperature that critically affects the cell performance.
5. For passive DMFC stacks, there is still plenty of scope to improve the current stack design to make the overall system more compact and achieve an effective management of heat, water and air under the operating condition of feeding a high-fuel concentration.

References

[1] X. Ren, T.E. Springer, T.A. Zawodzinski, et al., J. Electrochem. Soc. 147 (2000) 466.
[2] Q. Ye, T.S. Zhao, H. Yang, et al., Electrochem. Solid-State Lett. 8 (2005) A52.
[3] K. Scott, W.K. Taama, P. Argyropoulos, J. Power Sources 79 (1999) 43.
[4] J.B. Xu, T.S. Zhao, Z.X. Liang, et al., Chem. Mater. 20 (2008) 1688.
[5] C.Y. Du, T.S. Zhao, C. Xu, J. Power Sources 167 (2007) 265.
[6] Z. Qi, A. Kaufman, J. Power Sources 110 (2002) 177.
[7] H. Dohle, R. Jung, N. Kimiaie, et al., J. Power Sources 124 (2003) 371.
[8] J. Prabhuram, T.S. Zhao, Z.K. Tang, et al., J. Phys. Chem. B 110 (2006) 5245.
[9] G.Q. Lu, C.Y. Wang, T.J. Yern, et al., Electrochim. Acta 49 (2004) 821.
[10] H. Yang, T.S. Zhao, Q. Ye, J. Power Sources 139 (2005) 79.
[11] R. Jiang, D. Chu, J. Electrochem. Soc. 151 (1) (2004) A69.
[12] L.H. Jiang, G.Q. Sun, S.L. Wang, et al., Electrochem. Commun. 7 (2005) 663.
[13] C. Xu, T.S. Zhao, Y.L. He, J. Power Sources 171 (2007) 268.
[14] C.W. Wong, T.S. Zhao, Q. Ye, et al., J. Electrochem. Soc. 152 (2005) A600.
[15] S.H. Ge, X.G. Li, I.M. Hsing, J. Electrochem. Soc. 151 (2004) B523.
[16] C.K. Dyer, J. Power Sources 106 (2002) 31.
[17] W.W. Yang, T.S. Zhao, Electrochim. Acta 52 (2007) 6125.
[18] Z.X. Liang, T.S. Zhao, J. Phys. Chem. C 111 (2007) 8128.
[19] J.W. Guo, T.S. Zhao, J. Prabhuram, et al., Electrochim. Acta 51 (2005) 754.
[20] B.K. Kho, B. Bae, M.A. Scibioh, et al., J. Power Sources 142 (2005) 50.
[21] J.P. Esquivel, N. Sabaté, J. Santander, et al., Microsyst. Technol. 14 (2008) 535.
[22] H. Chang, J.R. Kim, J.H. Cho, et al., Solid State Ion. 148 (2002) 301.
[23] B.K. Kho, I.H. Oh, S.A. Hong, et al., Electrochim. Acta 50 (2004) 781.
[24] B. Bae, B.K. Kho, T.H. Lim, et al., J. Power Sources 158 (2006) 1256.
[25] C.Y. Chen, P. Yang, Y.S. Lee, et al., J. Power Sources 141 (2005) 24.
[26] Y.Q. Jiang, X.H. Wang, L.Y. Zhong, et al., J. Micromech. Microeng. 16 (2006) S233.
[27] V. Saarinen, O. Himanenb, T. Kallio, et al., J. Power Sources 172 (2007) 805.
[28] Q. Ye, T.S. Zhao, J. Power Sources 147 (2005) 196.
[29] J. Han, E.S. Park, J. Power Sources 112 (2004) 477.
[30] W. Lee, H. Kim, T.K. Kim, et al., J. Membr. Sci. 292 (2007) 29.
[31] V. Saarinen, O. Himanen, T. Kallio, et al., J. Power Sources 163 (2007) 768.
[32] G.G. Park, T.H. Yang, Y.G. Yoon, et al., Int. J. Hydrogen Energy 28 (2003) 645.
[33] J.G. Liu, G.G. Sun, F.L. Zhao, et al., J. Power Sources 133 (2004) 175.
[34] D. Kim, E.A. Cho, S.A. Hong, et al., J. Power Sources 130 (2004) 172.
[35] J.G. Liu, T.S. Zhao, Z.X. Liang, et al., J. Power Sources 153 (2006) 61.
[36] R. Chen, T.S. Zhao, J. Power Sources 167 (2007) 455.
[37] J.G. Liu, T.S. Zhao, R. Chen, et al., Electrochem. Commun. 7 (2005) 288.
[38] Z. Guo, A. Faghri, J. Power Sources 160 (2006) 1183.
[39] R. Chen, T.S. Zhao, J.G. Liu, J. Power Sources 157 (2006) 351.
[40] Q.Z. Lai, G.P. Yin, J. Zhang, et al., J. Power Sources 175 (2008) 458.
[41] W.M. Yang, S.K. Chou, C. Shua, J. Power Sources 164 (2007) 549.
[42] D. Chu, R.Z. Jiang, Electrochim. Acta 51 (2006) 5829.
[43] T. Shimizu, T. Momma, M. Mohamedi, et al., J. Power Sources 137 (2004) 277.
[44] H.K. Kim, J.M. Oh, J.H. Kim, et al., J. Power Sources 162 (2006) 497.
[45] N. Nakagawa, M.A. Abdelkareem, K. Sekimoto, J. Power Sources 160 (2006) 105.
[46] M.A. Abdelkareem, N. Nakagawa, J. Power Sources 162 (2006) 114.
[47] M.A. Abdelkareem, N. Morohashi, N. Nakagawa, J. Power Sources 172 (2007) 659.
[48] H.F. Zhang, I.M. Hsing, J. Power Sources 167 (2007) 450.
[49] W.J. Kim, H.G. Choi, Y.K. Lee, et al., J. Power Sources 157 (2006) 193.
[50] W.J. Kim, H.G. Choi, Y.K. Lee, et al., J. Power Sources 163 (2006) 98.
[51] Y.H. Pan, Electrochem. Solid-State Lett. 9 (2006) A349.
[52] A. Oedegaard, C. Hentschel, J. Power Sources 158 (2006) 177.
[53] Z. Guo, Y. Cao, J. Power Sources 132 (2004) 86.
[54] Z. Guo, A. Faghri, J. Power Sources 160 (2006) 1142.
[55] Y.M. Yang, Y.C. Liang, J. Power Sources 165 (2007) 185.
[56] Y.H. Chan, T.S. Zhao, R. Chen, et al., J. Power Sources 176 (2008) 183.
[57] H.K. Kim, J. Power Sources 162 (2006) 1232.
[58] Z. Guo, A. Faghri, J. Power Sources 167 (2007) 378.
[59] S. Eccariusa, F. Krausea, K. Beardb, et al., J. Power Sources 182 (2008) 565.
[60] E. Peled, A. Blum, A. Aharon, et al., Electrochem. Solid-State Lett. 6 (2003) A268.
[61] A. Blum, T. Duvdevani, M. Philosoph, et al., J. Power Sources 117 (2003) 22.
[62] G. Jewett, Z. Guo, A. Faghri, J. Power Sources 168 (2007) 434.
[63] K.Y. Song, H.K. Lee, H.T. Kim, Electrochim. Acta 53 (2007) 637.
[64] Y.H. Pan, J. Power Sources 161 (2006) 282.
[65] T.V. Reshetenko, H.T. Kim, H.J. Kweon, J. Power Sources 171 (2007) 433.
[66] T.V. Reshetenko, H.T. Kim, H.J. Kweon, Electrochim. Acta 53 (2008) 3043.
[67] R. Chen, T.S. Zhao, Electrochim. Acta 52 (2007) 4317.
[68] R. Chen, T.S. Zhao, Electrochem. Commun. 9 (2007) 718.
[69] C.Y. Chen, P. Yang, J. Power Sources 123 (2003) 37.
[70] J.J. Martin, W.M. Qian, H.J. Wang, et al., J. Power Sources 164 (2007) 287.
[71] Z. Guo, A. Faghri, Int. Commun. Heat Mass Transf. 35 (2008) 225.
[72] J.Y. Cao, Z.Q. Zou, Q.H. Huang, et al., J. Power Sources 185 (2008) 433.
[73] Y.J. Kim, B.C. Bae, M.A. Scibioh, et al., J. Power Sources 157 (2006) 253.
[74] V. Baglio, A. Stassi, F.V. Matera, et al., J. Power Sources 180 (2008) 797.
[75] S.W. Lim, S.W. Kim, H.J. Kim, et al., J. Power Sources 161 (2006) 27.
[76] Y.H. Chan, T.S. Zhao, R. Chen, et al., J. Power Sources 178 (2008) 118.
[77] J.J. Hwang, S.D. Wu, L.K. Lai, et al., J. Power Sources 161 (2006) 240.
[78] T.K. Yeh, C.H. Chen, J. Power Sources 175 (2008) 353.
[79] R. Chen, T.S. Zhao, J. Power Sources 152 (2005) 122.
[80] J. Rice, A. Faghri, Int. J. Heat Mass Transf. 49 (2006) 4804.
[81] J. Rice, A. Faghri, ASME J. Heat Transf. 130 (2008) 062001.
[82] B. Xiao, A. Faghri, Int. J. Heat Mass Transf. 51 (2008) 3127.
[83] J. Rice, A. Faghri, Int. J. Heat Mass Transf. 51 (2008) 948.
[84] R. Chen, T.S. Zhao, W.W. Yang, et al., J. Power Sources 175 (2008) 276.